

Article

Twenty-Nine New Limonoids with Skeletal Diversity from the Mangrove Plant, *Xylocarpus moluccensis*

Jianzhi Zhang ^{1,†}, Wanshan Li ^{1,†}, Yiguo Dai ¹, Li Shen ^{1,*}  and Jun Wu ^{2,*} 

¹ Marine Drugs Research Center, College of Pharmacy, Jinan University, 601 Huangpu Avenue West, Guangzhou 510632, China; jierzhang1990@163.com (J.Z.); mimowanshan@163.com (W.L.); 15521337878@163.com (Y.D.)

² School of Pharmaceutical Sciences, Southern Medical University, 1838 Guangzhou Avenue North, Guangzhou 510515, China

* Correspondence: shenli6052@sina.com or shenli6052@jnu.edu.cn (L.S.); wwujun2003@yahoo.com (J.W.); Tel.: +86-20-8522-2050 (L.S.)

† These authors contributed equally.

Received: 11 December 2017; Accepted: 17 January 2018; Published: 19 January 2018

Abstract: Twenty-nine new limonoids—named xylomolins A₁–A₇, B₁–B₂, C₁–C₂, D–F, G₁–G₅, H–I, J₁–J₂, K₁–K₂, L₁–L₂, and M–N, were isolated from the seeds of the mangrove plant, *Xylocarpus moluccensis*. Compounds **1**–**13** are mexicanolides with one double bond or two conjugated double bonds, while **14** belongs to a small group of mexicanolides with an oxygen bridge between C1 and C8. Compounds **15**–**19** are khayanolides containing a $\Delta^{8,14}$ double bond, whereas **20** and **21** are rare khayanolides containing a $\Delta^{14,15}$ double bond and $\Delta^{8,9}$, $\Delta^{14,15}$ conjugated double bonds, respectively. Compounds **22** and **23** are unusual limonoids possessing a (Z)-bicyclo[5.2.1]dec-3-en-8-one motif, while **24** and **25** are 30-ketophragmalins with $\Delta^{8,9}$, $\Delta^{14,15}$ conjugated double bonds. Compounds **26** and **27** are phragmalin 8,9,30-ortho esters, whereas **28** and **29** are azadirone and andirobin derivatives, respectively. The structures of these compounds, including absolute configurations of **15**–**19**, **21**–**23**, and **26**, were established by HRESIMS, extensive 1D and 2D NMR investigations, and the comparison of experimental electronic circular dichroism (ECD) spectra. The absolute configuration of **1** was unequivocally established by single-crystal X-ray diffraction analysis, obtained with Cu K α radiation. The diverse cyclization patterns of **1**–**29** reveal the strong flexibility of skeletal plasticity in the limonoid biosynthesis of *X. moluccensis*. Compound **23** exhibited weak antitumor activity against human triple-negative breast MD-MBA-231 cancer cells with an IC₅₀ value of 37.7 μ M. Anti-HIV activities of **1**, **3**, **8**, **10**, **11**, **14**, **20**, **23**–**25**, and **27** were tested in vitro. However, no compounds showed potent inhibitory activity.

Keywords: mangrove; *Xylocarpus moluccensis*; limonoid; xylomolins; skeletal diversity; antitumor; anti-HIV

1. Introduction

Limonoids are highly oxidized tetranortriterpenoids from a biosynthetic precursor with a 4,4,8-trimethyl-17-furanylsteroid skeleton. This group of natural products has attracted considerable attention because of its abundance, fascinating structural diversity, and various biological activities [1–4]. *Xylocarpus* is a well-known genus of mangrove plants which has been found to produce various types of limonoids with a broad range of bioactivities, such as insect antifeedant, antitumor, neuroprotective, gastroprotective, and antidepressant-like activities [5–11]. *X. moluccensis*, a true mangrove tree, is mainly distributed in Bangladesh, India, Indochina, Malesia, and tropical Australia. Previous chemical investigations of *X. moluccensis* resulted in the isolation of more than 100 limonoids with diverse carbon skeletons, such as mexicanolide, phragmalin, gedunin, andirobin,

and khayanolide compounds [12–18]. Limonoids with diverse skeletons from *X. moluccensis* revealed structural plasticity in the limonoid biosynthesis of this mangrove species. This inference drove us to obtain and identify more novel and bioactive limonoids from this mangrove plant.

Further investigation of the seeds of *X. moluccensis* afforded fourteen mexicanolides (1–14), seven khayanolides (15–21), two unusual limonoids with a (*Z*)-bicyclo[5.2.1]dec-3-en-8-one substructure (22, 23), two 30-ketophragmalins (24, 25), two phragmalin 8,9,30-*ortho* esters (26, 27), an azadirone derivative (28), and an andirobin derivative (29) (Figure 1). Herein, we report the isolation, structural identification, antitumor, and anti-HIV activities of these new limonoids.

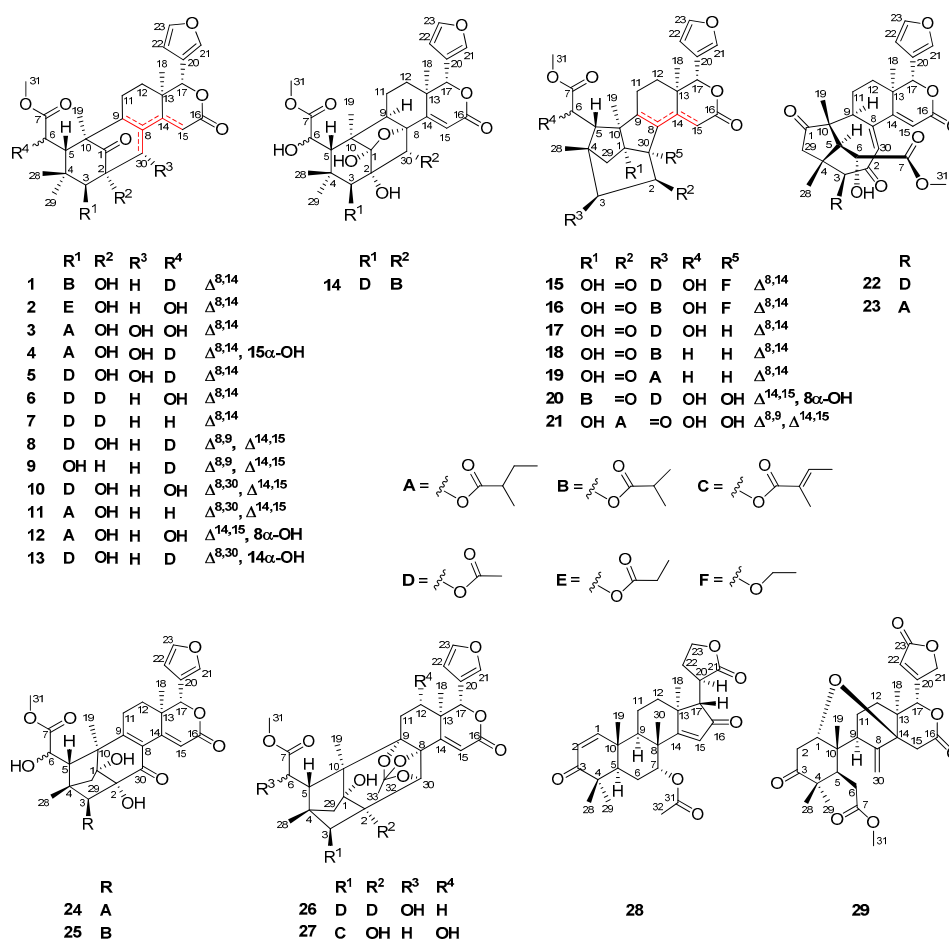


Figure 1. Structures of compounds 1–29.

2. Results and Discussion

In this paper, 16 compounds (*viz.* 1, 3–6, 8, 9, 12–14, 20, 21, 24, 26, 27, and 29) were obtained from seeds of the Thai *X. moluccensis*, whereas 13 compounds (*viz.* 2, 7, 10, 11, 15–19, 22, 23, 25, and 28) were isolated from those of the Indian *X. moluccensis*.

Compound 1 was obtained as a colorless crystal. The molecular formula of 1 was established from the positive HRESIMS ion peak at m/z 615.2785 (calcd. for $[M + H]^+$, 615.2800) to be $C_{33}H_{42}O_{11}$, implying thirteen degrees of unsaturation. According to the 1H and ^{13}C NMR spectroscopic data (Tables 1 and 2), five elements of unsaturation were due to four ester groups, a keto carbonyl function, and three carbon-carbon double bonds; thus, the molecule was pentacyclic. The 1H and ^{13}C NMR spectroscopic data (Tables 1 and 2) showed the presence of a β -substituted furan ring [δ_H 7.52 br d ($J = 0.8$ Hz H-21), 6.45 br d ($J = 1.2$ Hz H-22), 7.44 t ($J = 1.6$ Hz H-23)], four tertiary methyl groups (δ_H 1.27 s H₃-19, 1.04 s H₃-29, 1.05 s H₃-18, 0.84 s H₃-28), a methoxy (δ_H 3.73 s H₃-31), and a keto function (δ_C 216.7 qC), indicating a mexicanolide-type limonoid for 1.

The NMR spectroscopic data of **1** (Tables 1 and 2) were similar to those of khayalenoid H [19], except for the replacement of the 3-*O*-acetyl group in khayalenoid H by an isobutyryloxy group [δ_{H} 2.64 m 1H, 1.22 d ($J = 7.2$ Hz 3H), 1.24 d ($J = 7.2$ Hz 3H); δ_{C} 175.9 qC, 34.5 CH, 19.9 CH₃, 18.4 CH₃] in **1**. The presence of the isobutyryloxy group was corroborated by ¹H-¹H COSY correlations between H₃-34/H-33 and H₃-35/H-33. The significant HMBC correlation from H-3 (δ_{H} 4.97 s) to the carbonyl carbon (δ_{C} 175.9 qC) of the isobutyryloxy group placed it at C-3 (Figure 2a).

The relative configuration of **1** was established by diagnostic NOE interactions (Figure 2b). Those between H-17/H-11 β , H-17/H-12 β , H-17/H-5, and H-5/H₃-28 revealed their cofacial relationship, and were arbitrarily assigned as the β -oriented H-17 and H-5. NOE interactions between H-9/H-12 α , H-9/H₃-19, H₃-18/H-12 α , H-3/H₃-29, and 2-OH/H₃-29 assigned the α -orientation for H-9, H₃-18, H₃-19, H-3, and 2-OH.

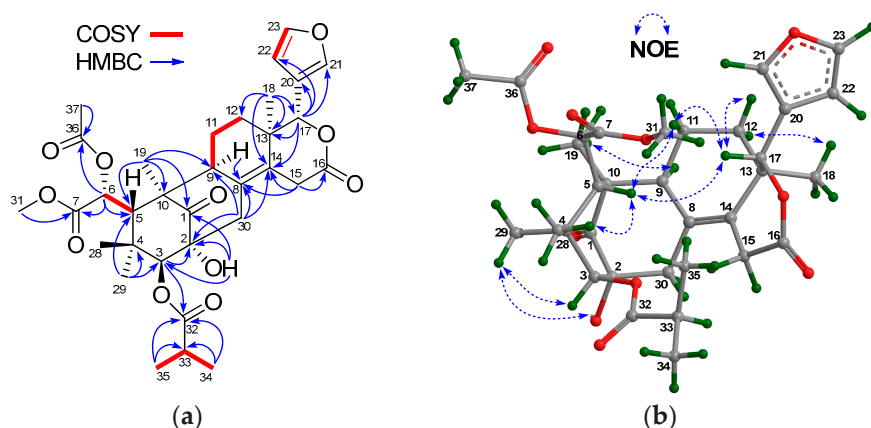


Figure 2. (a) Selected ¹H-¹H COSY and HMBC correlations for compound **1** (measured in CDCl₃); (b) Diagnostic NOE interactions for compound **1** (measured in CDCl₃, crystal structure of X-ray diffraction).

In order to establish the absolute configuration of **1**, single-crystal X-ray diffraction analysis with Cu K α radiation (Flack parameter of -0.06 (10), Flack x of -0.14 (11), and Hooft y of -0.04 (3); suitable crystals of **1** were obtained from acetone/methanol (1:2) at room temperature) was employed, which unequivocally assigned the absolute configuration of **1** as 2*R*,3*S*,5*S*,6*R*,9*S*,10*R*,13*R*,17*R*. The computer-generated perspective drawing of the X-ray structure of **1** is shown in Figure 3. Therefore, the absolute configuration of **1** named xylomolin A₁ was assigned as shown (Figure 2a).

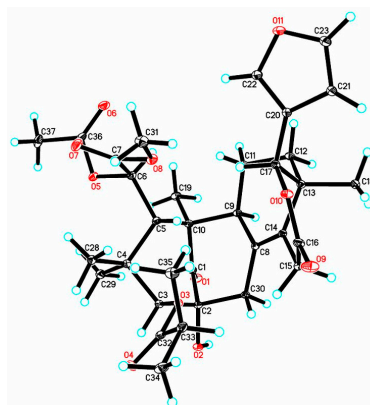


Figure 3. Oak Ridge Thermal-Ellipsoid Plot Program (ORTEP) illustration of the X-ray structure of compound **1**. Ellipsoids are given at the 30% probability level.

Table 1. ^1H NMR spectroscopic data (400 MHz, in CDCl_3) of compounds 1–7 (δ in ppm, J in Hz).

Position	1	2	3	4	5	6	7
3	4.97 s	4.93 s	5.04 s	5.12 s	5.06 s	5.19 s	5.52 s
5	3.35 s	3.13 s	3.28 s	3.47 s	3.45 s	3.09 s	3.10 br d (10.8)
6 α	5.47 s	4.52 br s	4.54 s	5.44 s	5.47 s	4.52 s	2.32 dd (16.5, 1.6)
6 β							2.42 dd (16.5, 10.7)
9	2.10 br s	2.14 br s	2.46 br s	2.49 br d (6.0)	2.42 br s	2.17 br s	2.08 m
11 α	1.80 m	1.84 m	1.85 m	1.84 m	1.84 m	1.82 m	1.74 m
11 β	1.92m	1.84 m	1.91 m	1.99 m	1.94 m	1.82 ¹	1.81 m
12 β	1.81 m	1.72 m	1.74 m	1.86 m	1.85 m	1.71 m	1.75 m
12 α	1.18 m	1.24 m	1.23 m	1.13 m	1.22 m	1.17 m	1.13 m
15 α	3.46 dt (20.8, 2.8)	3.47 dt (20.8, 3.2)	3.64 dd (20.8, 3.2)	5.23 d (2.4)	3.65 dd (20.8, 3.2)	3.51 dt (20.8, 3.2)	3.52 dt (20.8, 2.8)
15 β	3.79 d (20.8)	3.77 d (20.8)	3.85 br d (20.8)		3.81 br d (20.8)	3.88 br d (20.8)	3.88 d (20.8)
17	5.58 s	5.53 s	5.50 s	5.50 s	5.57 s	5.56 s	5.73 s
18	1.05 s	1.03 s	1.09 s	1.06 s	1.12 s	1.05 s	1.09 s
19	1.27 s	1.52 s	1.51 s	1.26 s	1.26 s	1.49 s	1.23 s
21	7.52 br d (0.8)	7.47 br d (0.8)	7.50 br s	7.59 t (0.8)	7.57 br s	7.47 br d (0.8)	7.54 br s
22	6.45 br d (1.2)	6.41 br d (0.8)	6.42 br d (1.2)	6.50 br d (1.2)	6.48 br d (1.2)	6.41 br t (0.8)	6.47 br d (1.2)
23	7.44 t (1.6)	7.43 t (1.6)	7.44 t (1.6)	7.45 t (1.6)	7.44 t (1.6)	7.43 t (1.6)	7.42 br d (1.6)
28	0.84 s	0.78 s	0.78 s	0.82 s	0.82 s	0.79 s	0.71 s
29	1.04 s	1.05 s	1.06 s	1.09 s	1.05 s	1.21 s	0.97 s
30 β	3.23 d (14.4)	3.21 d (14.8)	4.69 s	5.00 s	4.69 s	3.72 d (14.4)	3.47 d (14.8)
30 α	1.79 ¹	1.78 m				2.06 br d (14.4)	2.07 ¹
7-OMe-31 3-OAcyl	3.73 s	3.83 s	3.83 br s	3.75 s	3.76 s	3.84 s	3.70 s
33	2.64 m	2.45 m 2.43 m	2.38 m	2.27 m	2.17 s	2.20 s	2.22 s
34	1.22 d (7.2)	1.20 t (7.6)	1.50 m 1.80 m	1.49 m 1.80 m	6-Acyl	2-Acyl	2-Acyl
35	1.24 d (7.2)		0.99 t (7.2)	0.95 t (7.2)	2.18 s	2.13 s	2.12 s
36	6-Acyl		1.19 d (7.2)	1.20 d (7.2)			
37	2.19 s			6-Acyl			
38				2.18 s			
2-OH	4.12 br s	4.16 s	4.62 s	4.22 s	4.57 br s		
6-OH		2.80 br s	2.85 s			2.80 br s	
15-OH				3.66 br s			
30-OH			2.77 br s	2.58 br s	2.67 br s		

¹ Overlapped signals assigned by ^1H - ^1H COSY, HSQC, and HMBC spectra without designating multiplicity.**Table 2.** ^{13}C NMR spectroscopic data (100 MHz, in CDCl_3) of compounds 1–7 (δ in ppm).

Position	1	2	3	4	5	6	7
1	216.7 qC	217.2 qC	213.8 qC	212.7 qC	213.1 qC	209.4 qC	209.6 qC
2	78.0 qC	77.8 qC	79.4 qC	79.3 qC	79.5 qC	85.6 qC	85.8 qC
3	86.1 CH	86.7 CH	86.3 CH	85.2 CH	86.4 CH	83.4 CH	81.3 CH
4	39.7 qC	39.5 qC	39.9 qC	39.9 qC	39.8 qC	40.4 qC	40.1 qC
5	44.2 CH	45.1 CH	45.7 CH	44.7 CH	44.8 CH	44.7 CH	40.7 CH
6	72.7 CH	73.1 CH	73.0 CH	72.6 CH	72.7 CH	73.2 CH	33.3 CH ₂
7	171.1 qC	175.2 qC	175.1 qC	171.5 qC	171.2 qC	175.2 qC	174.1 qC
8	125.7 qC	126.6 qC	128.6 qC	135.4 qC	127.6 qC	126.2 qC	125.5 qC
9	52.9 CH	53.3 CH	47.4 CH	46.0 CH	46.9 CH	53.1 CH	52.3 CH
10	52.4 qC	52.4 qC	51.8 qC	52.5 qC	51.9 qC	53.4 qC	53.2 qC
11	18.7 CH ₂	18.9 CH ₂	18.4 CH ₂	17.9 CH ₂	18.2 CH ₂	18.9 CH ₂	18.7 CH ₂
12	29.4 CH ₂	29.6 CH ₂	29.1 CH ₂	27.8 CH ₂	28.8 CH ₂	29.5 CH ₂	29.1 CH ₂
13	38.3 qC	38.2 qC	38.5 qC	39.4 qC	38.6 qC	38.2 qC	38.3 qC
14	133.5 qC	132.6 qC	137.8 qC	140.1 qC	138.5 qC	133.2 qC	133.4 qC

Table 2. Cont.

Position	1	2	3	4	5	6	7
15	33.4 CH ₂	33.6 CH ₂	32.8 CH ₂	65.4 CH	32.8 CH ₂	33.6 CH ₂	33.5 CH ₂
16	169.2 qC	169.3 qC	168.9 qC	173.6 qC	169.2 qC	169.3 qC	169.9 qC
17	80.8 CH	80.8 CH	80.7 CH	81.1 CH	80.6 CH	80.6 CH	80.3 CH
18	18.0 CH ₃	18.3 CH ₃	17.7 CH ₃	16.1 CH ₃	17.6 CH ₃	18.4 CH ₃	18.1 CH ₃
19	16.7 CH ₃	17.6 CH ₃	17.6 CH ₃	17.0 CH ₃	16.8 CH ₃	17.8 CH ₃	16.9 CH ₃
20	120.5 qC	120.6 qC	120.5 qC	119.8 qC	120.3 qC	120.6 qC	120.5 qC
21	141.5 CH	141.1 CH	141.2 CH	141.9 CH	141.7 CH	141.2 CH	141.8 CH
22	109.8 CH	109.7 CH	109.7 CH	109.8 CH	109.9 CH	109.7 CH	109.9 CH
23	143.1 CH	143.2 CH	143.2 CH	143.2 CH	143.1 CH	143.2 CH	142.9 CH
28	22.5 CH ₃	22.6 CH ₃	22.8 CH ₃	22.5 CH ₃	22.7 CH ₃	22.6 CH ₃	22.8 CH ₃
29	22.7 CH ₃	22.6 CH ₃	22.7 CH ₃	22.7 CH ₃	22.6 CH ₃	23.5 CH ₃	21.1 CH ₃
30	44.4 CH ₂	44.6 CH ₂	73.0 CH	73.6 CH	72.9 CH	40.1 CH ₂	40.3 CH ₂
31	53.2 CH ₃	53.2 CH ₃	53.3 CH ₃	53.3 CH ₃	53.3 CH ₃	53.3 CH ₃	52.2 CH ₃
	3-Acyl						
32	175.9 qC	173.3 qC	175.5 qC	175.3 qC	169.7 qC	169.6 qC	169.6 qC
33	34.5 CH	28.0 CH ₂	41.2 CH	41.8 CH	21.2 CH ₃	21.2 CH ₃	21.3 CH ₃
					6-Acyl	2-Acyl	2-Acyl
34	19.9 CH ₃	9.4 CH ₃	26.1 CH ₂	26.5 CH ₂	169.7 qC	169.1 qC	169.0 qC
35	18.4 CH ₃		11.6 CH ₃	11.8 CH ₃	21.0 CH ₃	21.8 CH ₃	21.7 CH ₃
36			17.5 CH ₃	17.5 CH ₃			
	6-Acyl			6-Acyl			
37	169.7 qC			169.8 qC			
38	21.0 CH ₃			21.0 CH ₃			

Compound **2** was obtained as an amorphous white powder. The molecular formula was determined to be C₃₀H₃₈O₁₀ by the negative HRESIMS ion peak at m/z 593.2143 (calcd. for [M + Cl][−], 593.2159). The NMR spectroscopic data of **2** resembled those of **1** (Tables 1 and 2), except for the replacement of the 3-*O*-isobutyryl moiety and the 6-*O*-acetyl group in **1** by a 3-*O*-propionyl moiety (δ_{H} 2.45 m 1H, 2.43 m 1H, 1.20 t ($J = 7.6$ Hz 3H); δ_{C} 173.3 qC, 28.0 CH₂, 9.4 CH₃) and a 6-OH group in **2**, respectively. The presence of a 3-*O*-propionyl moiety was confirmed by ¹H-¹H COSY correlations between H₃-34/H₂-33 and HMBC cross-peaks between H₃-34/C-33, H₃-34/C-32, H₂-33/C-32, and H-3/C-32. The relative configuration of **2** (except for that of C-6) was determined to be the same as that of **1** by NOE interactions between H-17/H-15 β , H-15 β /H-30 β , H-17/H-12 β , H-17/H-11 β , H-11 β /H-5, H-17/H-5, and H-5/H₃-28, and those between H-9/H₃-19, H₃-19/H₃-29, H₃-29/H-3, and H₃-18/H-15 α . Thus, the structure of **2**—named xylomolin A₂—was assigned as shown in Figure 1.

Compound **3** gave the molecular formula C₃₂H₄₂O₁₁ as established by the HRESIMS ion peak at m/z 625.2620 (calcd. for [M + Na]⁺, 625.2619). The NMR spectroscopic data of **3** (Tables 1 and 2) were similar to those of moluccensin S [20], except for the presence of an additional 30-OH group, which was supported by the downshifted C-30 signal (δ_{C} 73.0 CH in **3**, whereas δ_{C} 44.6 CH₂ in moluccensin S) and HMBC correlations from the proton of 30-OH to C-30, C-2, and C-8. NOE interactions between H-17/H-12 β , H-17/H-11 β , H-5/H-12 β , H-5/H-17, H-5/H₃-28, and H-5/H-30 revealed the β -orientation for H-5, H-17, H-30, and H₃-28, and the corresponding 30 α -OH. Similarly, those between H-3/2-OH, H₃-29/2-OH, H-9/H₃-19, H₃-29/H₃-19, and H₃-18/H-11 α assigned the α -orientation for H-3, H-9, H₃-18, H₃-19, H₃-29, and 2-OH. Thus, the structure of **3**—named xylomolin A₃—was determined to be 30 α -hydroxy-moluccensin S.

Compound **4** provided the molecular formula of C₃₄H₄₄O₁₃ as determined from the positive HRESIMS ion peak at m/z 683.2675 (calcd. for [M + Na]⁺, 683.2674). The ¹H and ¹³C NMR spectroscopic data of **4** resembled those of **3** (Tables 1 and 2), the difference being the presence of a 15-OH function (δ_{H} 3.66 br s) and a 6-acetoxy group (δ_{H} 2.18 s 3H; δ_{C} 169.8 qC, 21.0 CH₃) in **4**. The existence of a 15-OH function was corroborated by the downshifted C-15 signal (δ_{C} 65.4 CH in **4**, whereas δ_{C}

32.8 CH₂ in **3**) and HMBC correlations from the proton of 15-OH to C-14, C-15, and C-16. The HMBC correlation from H-6 to the carbonyl carbon (C-37) of the acetoxy group placed it at C-6. The relative configuration of **4** (except that of C-15) was assigned as the same as that of **3** on the basis of NOE interactions. Those between H-17/H-15 and H-5/H-30 assigned the β -oriented H-15 and H-30, and the corresponding 15 α -OH group. Consequently, the structure of **4**—named xylomolin A₄—was identified as 15 α -hydroxy-6-acetoxy-xylomolin A₃.

The molecular formula of **5** was determined to be C₃₁H₃₈O₁₂ by the positive HRESIMS ion peak at m/z 625.2252 (calcd. for [M + Na]⁺, 625.2255). The ¹H and ¹³C NMR spectroscopic data of **5** (Tables 1 and 2) were closely related to those of khayalenoid H, the difference being the existence of a 30-OH function, which was supported by the downshifted C-30 signal (δ_C 72.9 CH in **5**, whereas δ_C 44.4 CH₂ in khayalenoid H). HMBC correlations from the proton of 30-OH (δ_H 2.67 br s) to C-30 and C-8 demonstrated the above deduction. The NOE interaction between H-5/H-30 assigned the β -oriented H-30 and the corresponding 30 α -OH. Thus, the structure of **5**—named xylomolin A₅—was assigned as 30 α -hydroxy-khayalenoid H.

Compound **6** was isolated as a white and amorphous powder. Its molecular formula was determined to be C₃₁H₃₈O₁₁ from the positive HRESIMS ion peak at m/z 609.2311 (calcd. for [M + Na]⁺, 609.2306). The ¹H and ¹³C NMR spectroscopic data of **6** (Tables 1 and 2) closely resembled those of khayalenoid H [19], except for the replacement of the 2-OH function and the 6-O-acetyl group in khayalenoid H by a 2-O-acetyl (δ_H 2.13 s 3H; δ_C 169.1 qC, 21.8 CH₃) and a 6-OH group (δ_H 2.80 br s) in **6**, respectively. HMBC correlations from the proton of the 6-OH group to C-5, C-6, and C-7 placed it at C-6. The presence of the 2-O-acetyl group in **6** was corroborated by the downshifted C-2 in **6** (δ_C 86.5 qC in **6**, whereas δ_C 77.9 qC in khayalenoid H). HMBC correlations from H₂-30 and H-3 to C-2 confirmed the above deduction. The relative configuration of **6** was determined to be the same as that of khayalenoid H based on diagnostic NOE interactions between H-17/H-15 β , H-17/H-12 β , H-17/H-5, and H-5/H₃-28 and those between H-9/H₃-19, H₃-19/H₃-29, and H₃-18/H-15 α . Therefore, the structure of **6**—named xylomolin A₆—was determined to be 2-O-acetyl-6-O-deacetyl-khayalenoid H.

The molecular formula of **7** was determined to be C₃₁H₃₈O₁₀ by the positive HRESIMS ion peak at m/z 593.2358 (calcd. for [M + Na]⁺, 593.2357). The ¹H and ¹³C NMR spectroscopic data of **7** (Tables 1 and 2) were closely related to those of **6**, except for the absence of the 6-OH group, which was corroborated by the upshifted CH₂-6 signal (δ_H 2.32 dd (J = 16.5, 1.6 Hz), 2.42 dd (J = 16.5, 10.7 Hz), δ_C 33.3) in **7**. ¹H-¹H COSY correlations between H₂-6/H-5 and HMBC cross-peaks from H₂-6 and C-5 and C-7 confirmed the above result. The analysis of diagnostic NOE interactions revealed that **7** possessed the same relative configuration as that of **6**. Therefore, the structure of **7**—named xylomolin A₇—was assigned as 6-dehydroxy-xylomolin A₆.

Compound **8** was isolated as a white and amorphous powder. It had a molecular formula of C₃₁H₃₆O₁₁ as deduced from the positive HRESIMS ion peak at m/z 607.2151 (calcd. for [M + Na]⁺, 607.2150). The ¹H and ¹³C NMR spectroscopic data of **8** (Tables 3 and 4) were similar to those of heytrijunolide E [21] with $\Delta^{8,9}$ and $\Delta^{14,15}$ conjugated double bonds, except for the absence of the 15-OH group and the presence of an acetoxy group at C-3 in **8**. The absence of the 15-OH group was confirmed by the upshifted C-15 signal (δ_C 111.6 qC in **8**, whereas δ_C 134.7 qC in heytrijunolide E) and HMBC correlations between H-15/C-14, H-15/C-16, H-15/C-8, and H-15/C-13. The HMBC correlation from H-3 (δ_H 5.51 s) to the carbonyl carbon (δ_C 170.2 qC) of the acetoxy group placed it at C-3. The relative configuration of **8** was established to be the same as that of heytrijunolide E based on diagnostic NOE interactions between H₃-28/H-5, H-5/H-11 β , H-12 β /H-17, H₃-29/H-3, H-12 α /H₃-18, and H-11 α /H₃-19. Therefore, the structure of **8**—named xylomolin B₁—was assigned as 15-dehydroxy-3 β -acetoxy-heytrijunolide E.

Table 3. ¹H NMR spectroscopic data (400 MHz) of compounds 8–14 (δ in ppm, J in Hz).

Position	8 ¹	9 ¹	10 ¹	11 ¹	12 ²	13 ¹	14 ¹
2		3.02 t (6.0)					
3	5.51 s	4.26 d (6.0)	4.83 s	4.99 s	4.55 s	4.76 s	4.55 s
5	2.98 s	2.94 br s	3.12 s	3.20 dd (9.2, 3.2)	3.22 s	3.49 s	2.67 s
6	5.51 s	5.47 s	4.38 s	2.32 m 2.35 m	4.40 d (4.8)	5.55 s	4.20 br s
9			2.29 dt (12.4, 2.8)	2.29 m	1.71 t (13.2)	2.81 m	2.30 ³
11α	2.38 m	2.35 m	1.84 m	1.77 m	1.68 m	1.78 m	1.83 m
11β	2.38 ³	2.35 ³	1.38 qd (12.8, 4.4)	1.56 m	1.33 m	2.18 m	2.30 m
12β	1.46 m	1.45 m	2.00 m	1.93 m	1.85 d (14.0)	1.44 m	1.95 m
12α	1.65 m	1.61 m	1.24 td (13.6, 4.4)	1.29 m	1.19 m	2.05 m	1.41 m
15α	5.90 s	5.89 s	6.28 s	6.32 s	5.99 s	2.93 d (18.0)	6.08 s
15β						3.05 d (18.0)	
17	5.10 s	5.09 s	5.12 s	5.16 s	5.25 s	5.61 s	4.84 s
18	1.01 s	1.00 s	1.06 s	1.06 s	1.16 s	1.05 s	1.24 s
19	1.30 s	1.17 s	1.54 s	1.28 s	1.29 s	1.28 s	1.43 s
21	7.50 br s	7.49 br s	7.52 br s	7.51 br s	7.85 br s	7.76 br s	7.48 br t (0.8)
22	6.45 br d (1.2)	6.45 br d (1.2)	6.50 br d (1.2)	6.49 br d (1.2)	6.60 br d (1.2)	6.48 br s	6.42 br d (1.2)
23	7.46 t (1.6)	7.45 t (1.6)	7.45 t (1.6)	7.44 t (1.6)	7.70 t (1.6)	7.45 br s	7.42 t (1.6)
28	1.20 s	1.17 s	0.81 s	0.74 s	0.69 s	0.92 s	0.84 s
29	1.01 s	1.13 s	1.09 s	0.82 s	1.04 s	1.07 s	1.59 s
30β	3.55 d (17.6)	3.29 d (17.6)	6.29 d (4.4)	6.31 d (4.4)	3.38 d (15.6)	5.60 d (2.0)	5.49 s
30α	2.42 br d (17.6)	2.52 br d (17.6)			2.31 d (15.6)		
31	3.74 s	3.75 s	3.84 s	3.69 s	3.65 s	3.73 s	3.88 s
	3-Acyl	6-Acyl	3-Acyl	3-Acyl	3-Acyl	3-Acyl	3-Acyl
33	2.21 s	2.07 s	2.22 s	2.57 m	2.54 m	2.11 s	2.02 s
34	6-Acyl			1.61 m 1.81 m	1.60 m 1.54 m	6-Acyl	30-Acyl
35	2.11 s			1.04 t (7.2)	0.93 t (7.2)	2.19 s	2.59 m
36				1.25 d (6.8)	1.12 d (6.8)		1.13 d (6.8)
37							1.17 d (6.8)
1-OH							4.55 ³
2-OH			4.07 br s		5.08 s	4.17 br s	4.11 br s
6-OH			2.97 br s		5.58 d (4.8)		2.93 s
8-OH					5.05 s		

¹ Recorded in CDCl₃; ² Recorded in DMSO-*d*₆; ³ Overlapped signals assigned by ¹H-¹H COSY, HSQC, and HMBC spectra without designating multiplicity.

Table 4. ¹³C NMR spectroscopic data (100 MHz) of compounds 8–14 (δ in ppm).

Position	8 ¹	9 ¹	10 ¹	11 ¹	12 ²	13 ¹	14 ¹
1	211.1 qC	212.5 qC	212.0 qC	212.7 qC	215.9 qC	213.9 qC	108.4 qC
2	76.9 qC	50.5 CH	77.5 qC	77.4 qC	76.2 qC	76.9 qC	81.1 qC
3	81.6 CH	76.7 CH	87.2 CH	85.5 CH	86.5 CH	85.8 CH	85.6 CH
4	39.6 qC	39.7 qC	39.9 qC	39.7 qC	39.5 qC	39.4 qC	38.8 qC
5	55.0 CH	55.4 CH	44.8 CH	40.8 CH	44.6 CH	44.8 CH	44.6 CH
6	69.8 CH	70.2 CH	72.0 CH	32.7 CH ₂	71.2 CH	72.4 CH	71.7 CH
7	170.6 qC	170.9 qC	175.5 qC	173.5 qC	175.7 qC	171.0 qC	175.9 qC

Table 4. Cont.

Position	8 ¹	9 ¹	10 ¹	11 ¹	12 ²	13 ¹	14 ¹
8	126.1 qC	127.1 qC	134.7 qC	134.1 qC	71.3 qC	138.8 qC	80.0 qC
9	148.4 qC	150.3 qC	55.3 CH	53.8 CH	61.6 CH	53.3 CH	51.5 CH
10	51.9 qC	51.2 qC	53.2 qC	52.6 qC	48.4 qC	49.8 qC	43.1 qC
11	22.3 CH ₂	22.2 CH ₂	22.5 CH ₂	21.5 CH ₂	20.7 CH ₂	20.3 CH ₂	15.6 CH ₂
12	29.7 CH ₂	29.7 CH ₂	33.3 CH ₂	32.4 CH ₂	32.5 CH ₂	28.3 CH ₂	25.2 CH ₂
13	36.8 qC	36.8 qC	37.6 qC	37.5 qC	37.8 qC	41.0 qC	38.8 qC
14	156.4 qC	157.4 qC	160.7 qC	160.0 qC	168.3 qC	72.9 qC	158.3 qC
15	111.6 CH	110.6 CH	113.4 CH	113.2 CH	114.6 CH ₂	38.9 CH ₂	118.4 CH
16	165.2 qC	165.7 qC	164.8 qC	164.6 qC	164.3 qC	168.4 qC	163.1 qC
17	80.6 CH	80.7 CH	79.7 CH	79.7 CH	78.5 CH	77.2 CH	81.4 CH
18	16.2 CH ₃	16.1 CH ₃	22.5 CH ₃	21.9 CH ₃	22.6 CH ₃	15.7 CH ₃	19.5 CH ₃
19	18.2 CH ₃	18.3 CH ₃	16.2 CH ₃	15.6 CH ₃	18.5 CH ₃	15.7 CH ₃	22.1 CH ₃
20	119.8 qC	119.9 qC	120.0 qC	120.1 qC	120.0 qC	120.1 qC	119.9 qC
21	141.2 CH	141.2 CH	141.4 CH	141.5 CH	142.3 CH	141.7 CH	141.3 CH
22	109.9 CH	110.0 CH	110.2 CH	110.2 CH	110.6 CH	109.8 CH	109.9 CH
23	143.2 CH	143.1 CH	143.3 CH	143.2 CH	143.2 CH	143.1 CH	143.0 CH
28	26.3 CH ₃	25.6 CH ₃	21.4 CH ₃	21.5 CH ₃	21.7 CH ₃	22.0 CH ₃	24.0 CH ₃
29	28.0 CH ₃	28.3 CH ₃	23.0 CH ₃	20.8 CH ₃	24.8 CH ₃	22.1 CH ₃	24.5 CH ₃
30	39.2 CH ₂	28.8 CH ₂	133.5 CH	133.0 CH	45.9 CH ₂	130.2 CH	74.9 CH
31	53.0 CH ₃	52.8 CH ₃	53.4 CH ₃	52.1 CH ₃	52.0 CH ₃	53.4 CH ₃	53.4 CH ₃
	3-Acyl	6-Acyl	3-Acyl	3-Acyl	3-Acyl	3-Acyl	3-Acyl
32	170.2 qC	169.2 qC	169.9 qC	176.0 qC	174.7 qC	170.7 qC	171.5 qC
33	20.9 CH ₃	20.5 CH ₃	20.7 CH ₃	41.4 CH	40.4 CH	20.4 CH	20.7 CH ₃
	6-Acyl					6-Acyl	30-Acyl
34	169.1 qC			26.9 CH ₂	26.4 CH	169.6 qC	176.0 qC
35	20.5 CH ₃			11.9 CH ₃	11.2 CH ₃	21.0 CH ₃	34.2 CH
36				17.0 CH ₃	16.5 CH ₃		19.0 CH ₃
37							19.1 CH ₃

¹ Recorded in CDCl₃; ² Recorded in DMSO-*d*₆.

Compound **9** provided the molecular formula C₂₉H₃₄O₉ as established by the positive HRESIMS ion peak at *m/z* 527.2273 (calcd. for [M + H]⁺, 527.2276). The ¹H and ¹³C NMR spectroscopic data of **9** (Tables 3 and 4) were similar to those of heytrijunolide E [21], the difference being the absence of the 2-OH and 15-OH groups in **9**, which was corroborated by the upshifted C-15 (δ_C 110.6 CH in **9**, whereas δ_C 134.7 qC in heytrijunolide E) and C-2 (δ_C 50.5 CH in **9**, whereas δ_C 78.2 qC in heytrijunolide E) signals. A proton (δ_H 3.02 t (*J* = 6.0 Hz)) exhibiting ¹H-¹H COSY correlations to H-3 and H-30 and HMBC cross-peaks to C-1, C-3, C-4, and C-30 was assigned as H-2. The existence of H-15 (δ_H 5.89 s) was further confirmed by its HMBC correlations to C-8, C-13, C-14, and C-16. The relative configuration of **9** was determined to be the same as that of heytrijunolide E based on diagnostic NOE interactions between H₃-28/H-5, H-5/H-11β, H-12β/H-17, H₃-29/H-3, H-12α/H₃-18, and H-11α/H₃-19. Thus, the structure of **9**—named xylomolin B₂—was assigned as 2,15-dedihydroxy-heytrijunolide E.

Compound **10** had a molecular formula of C₂₉H₃₄O₁₀ as determined from the positive HRESIMS ion peak at *m/z* 543.2238 (calcd. for [M + H]⁺, 543.2230). The NMR data of **10** (Tables 3 and 4) closely resembled those of moluccensin U [20], except for the replacement of the 3-*O*-(2-methyl)butyryl group in moluccensin U by an acetoxy group (δ_H 2.22 s 3H; δ_C 169.9 qC, 20.7 CH₃) in **10**. The significant HMBC cross-peak from H-3 (δ_H 4.83 s) to the carbonyl carbon of the above acetoxy group placed it at C-3. NOE interactions between H-11β/H-17, H-12β/H-17, H-11β/H-5, H-5/H₃-28, H-9/H₃-18, H-9/H₃-19, and H₃-29/H-3 revealed the same relative configuration of **10** as that of moluccensin U. Therefore, the structure of **10**—named xylomolin C₁—was assigned as 3-*O*-acetyl-3-de(2-methyl)butyryloxy-moluccensin U.

Compound **11** afforded the molecular formula C₃₂H₄₀O₉ as established by the positive HRESIMS ion peak at *m/z* 591.2570 (calcd. for [M + Na]⁺, 591.2565). The ¹H and ¹³C NMR spectroscopic

data of **11** (Tables 3 and 4) closely resembled those of swietmanin G [22], the difference being the replacement of the 3-isobutyryloxy group in swietmanin G by a 2-methylbutyryloxy group (δ_{H} 2.57 m 1H, 1.61 m 1H, 1.81 m 1H, 1.04 t ($J = 7.2$ Hz 3H), 1.25 d ($J = 6.8$ Hz 3H); δ_{C} 176.0 qC, 41.4 CH, 26.9 CH₂, 11.9 CH₃, 17.0 CH₃) in **11**. The deduction was confirmed by ¹H-¹H COSY correlations between H₃-36/H-33, H₃-35/H₂-34, and H₂-34/H-33, and HMBC correlations between H-3/C-32, H₃-35/C-34, H₃-35/C-33, H₃-36/C-33, H₃-36/C-32, and H₃-36/C-34. NOE interactions between H-12 β /H-17, H-17/H-11 β , H-5/H-11 β , H-5/H₃-28, H-9/H₃-18, H-9/H₃-19, and H₃-29/H-3 assigned the α -orientation for H-9, H₃-18, H₃-19, and H-3. Thus, the structure of **11**—named xylomolin C₂—was assigned as 3-O-(2-methyl)butyryl-3-deisobutyryloxy-swietmanin G.

Compound **12** had the molecular formula C₃₂H₄₂O₁₁ as determined from the positive HRESIMS ion peak at m/z 625.2612 (calcd. for [M + Na]⁺, 625.2619). The ¹H and ¹³C NMR spectroscopic data of **12** (Tables 3 and 4) were similar to those of moluccensin U [20], except for the absence of the $\Delta^{8,30}$ double bond and the presence of an 8-OH group. This finding was verified by the upshifted C-8 (δ_{C} 71.3 qC) and C-30 (δ_{C} 45.9 CH₂) signals as compared with those (δ_{C} 134.5 qC and 133.6 CH) of moluccensin U, respectively. The presence of the 8-OH group was confirmed by HMBC correlations from its proton to C-8, C-9, and C-30. NOE interactions between 8-OH/H-9 and 8-OH/H₃-18 assigned the α -orientation for the 8-OH group. The relative configuration of **12** (except that of C-8) was established to be identical to that of moluccensin U based on diagnostic NOE interactions between H-12 β /H-17, H-5/H₃-28, H-9/H₃-19, and H₃-29/H-3. Thus, the structure of **12**—named xylomolin D—was assigned as 8,30-dihydrogen-8 α -hydroxy-moluccensin U.

Compound **13** was obtained as an amorphous white powder. The molecular formula was determined to be C₃₁H₃₈O₁₂ by the positive HRESIMS ion peak at m/z 625.2250 (calcd. for [M + Na]⁺, 625.2255). The ¹H and ¹³C NMR spectroscopic data of **13** (Tables 3 and 4) were similar to those of **8**, except for the replacement of $\Delta^{8,9}$ and $\Delta^{14,15}$ conjugated double bonds in **8** by a $\Delta^{8,30}$ double bond (δ_{C} 138.8 qC C-8, 130.2 CH C-30) in **13**, and the presence of an additional 14-OH group. HMBC correlations between H₂-15/C-14, H₂-15/C-16, H₂-15/C-13, H-30/C-14, H-30/C-9, and H-9/C-8 demonstrated the above deduction. In order to establish the relative configuration of the 14-OH group in **13**, two possible 3D structures with a 14 α -OH and 14 β -OH groups, respectively, were simulated by using the ChemBio3D software (Figure 4). When the 14-OH group occupies α -orientation, the space distance between H-5/H-17 is around 2.4 Å (Figure 4a), implying the presence of a strong NOE interaction between these protons. On the contrary, when the 14-OH group occupies the β -orientation, the space distance between H-5/H-17 is around 5.8 Å (Figure 4b), indicating the absence of a NOE interaction between these protons. Quite evidently, the NOE interaction between H-5/H-17 could be utilized as an effective criterion to resolve the relative configuration of the 14-OH group. Thus, the orientation of the 14-OH group in **13** was assigned as α based on the strong NOE interaction between H-5/H-17. Furthermore, the relative configuration of the whole molecule of **13** (except that of C-14) was determined to be the same as that of **8** on the basis of NOE interactions between H₃-28/H-5, H-5/H-11 β , H-12 β /H-17, H₃-29/H-3, H-12 α /H₃-18, and H-11 α /H₃-19. Thus, the structure of **13**—named xylomolin E—was assigned as depicted.

Compounds **2–13** are analogues of **1**. From the point of view of biogenetic origins, these mexicanolides should possess the same absolute configurations of carbon skeletons as that of **1**. The absolute stereostructures of **2–13** are shown as in Figure 1.

The molecular formula of **14** was determined to be C₃₃H₄₂O₁₃ by the positive HRESIMS ion peak at m/z 669.2521 (calcd. for [M + Na]⁺, 669.2518). The NMR spectroscopic data of **14** (Tables 3 and 4) were similar to those of xylorumphiin H [23], being a mexicanolide containing a C1-O-C8 bridge, except for the presence of an additional $\Delta^{14,15}$ double bond (δ_{H} 6.08 s 1H; δ_{C} 158.3 qC, 118.4 CH) and an additional 6-OH function (δ_{H} 2.93 s) in **14**. The existence of the $\Delta^{14,15}$ double bond was corroborated by HMBC correlations between H₃-18/C-14, H-15/C-8, and H-15/C-16. The downshifted C-6 signal (δ_{C} 71.7 CH in **14**, whereas δ_{C} 32.3 CH₂ in xylorumphiin H), along with HMBC cross-peaks from H-6 to C-5 and C-7, supported the location of a hydroxy group at

C-6. Similar NOE interactions of **14** as those of xylorumphiin H suggested that both mexicanolides possessed the same relative configuration. Thus, the structure of **14**—named xylomolin F—was assigned as 6-hydroxy-14,15-dedihydrogen-xylorumphiin H.

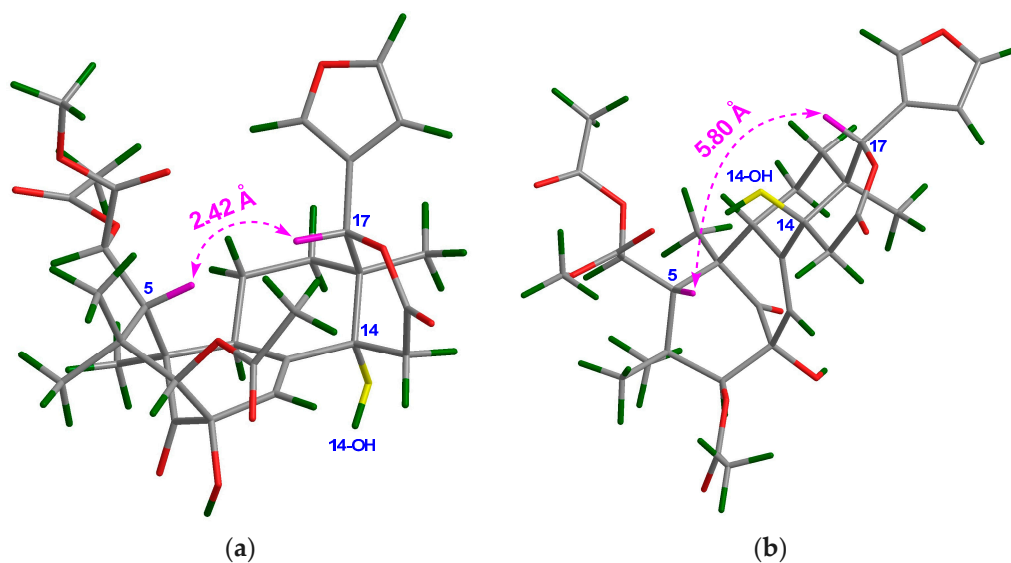


Figure 4. Molecular Mechanics, Allinger Force Field version 2 (MM2)-optimized two possible 3D structures for compound **13**. (a) The structure with a 14 α -OH group; (b) The structure with a 14 β -OH group.

The molecular formula of **15** was established by the positive HRESIMS ion peak at m/z 587.2494 (calcd. for $[M + H]^+$, 587.2492) to be $C_{31}H_{38}O_{11}$, implying thirteen degrees of unsaturation. According to the NMR spectroscopic data of **15** (Tables 5 and 6), seven elements of unsaturation were due to three carbon-carbon double bonds, one carbonyl group, and three ester functionalities; thus, **15** should be hexacyclic. The NMR spectroscopic data of **15** resembled those of thaixylomolin L [18], being a khayanolide isolated from seeds of the Thai *X. moluccensis*, except for the presence of an additional 6-OH group in **15**. Strong 3J HMBC correlations from H₂-29 to C-30 further confirmed a khayanolide for **15** instead of a phragmalin, which should exhibit weak 4J HMBC correlations between H₂-29/C-30. HMBC cross-peaks from an active proton (δ_H 2.91 d ($J = 3.4$ Hz)) to C-5 (δ_C 45.4, CH), C-6 (δ_C 72.0, CH), and C-7 (δ_C 175.3, qC) (Figure 5a) revealed the existence of a 6-OH group in **15**.

Table 5. ¹H NMR spectroscopic data (400 MHz) of compounds 15–21 (δ in ppm, *J* in Hz).

Position	15 ¹	16 ¹	17 ¹	18 ¹	19 ¹	20 ²	21 ¹
2							5.77 s
3	4.87 s	4.86 s	4.94 s	5.01 s	5.02 s	4.97 s	
5	2.24 br s	2.22 s	2.13 ³	2.24 dd (11.2, 2.4)	2.26 ³	2.87 s	2.19 br s
6	4.36 br s	4.37 br d (1.6)	4.33 s	2.27 dd (16.0, 2.8) 2.43 dd (16.0, 11.2)	2.28 dd (16.0, 2.8) 2.43 dd (16.0, 11.2)	4.83 br d (3.6)	4.42 s
9	2.52 m	2.51 m	2.51 m	2.45 m	2.46 m	2.49 dd (6.4, 2.8)	
11α	1.81 m	1.80 m	1.84 m	1.77 m	1.79 m	2.20 ³	2.25 m
11β	1.40 m	1.40 m	1.40 m	1.46 m	1.48 m	2.07 m	2.03 dd (18.8, 4.0)
12β	1.58 m	1.53 m	1.60 m	1.54 m	1.55 m	1.76 m	1.36 m
12α	1.43 m	1.43 m	1.47 m	1.43 m	1.44 m	1.27 m	1.51 overlapped
15α	3.71 ³	3.73 dd (20.0,3.2)	3.43 dd (19.2, 1.6)	3.43 br d (18.4)	3.43 dd (19.6, 1.2)	5.72 br s	6.55 s
15β	4.07 dd (20.0, 2.8)	4.09 dd (20.0,3.2)	3.98 dd (19.2, 3.2)	3.94 ddd (19.6, 3.6, 2.0)	3.93 ddd (19.6, 3.6, 2.0)		
17	5.13 s	5.06 s	5.18 s	5.17 s	5.14 s	5.66 s	5.09 s
18	1.05 s	1.04 s	1.04 s	1.01 s	1.01 s	1.38 s	1.00 s
19	1.34 s	1.34 s	1.29 s	1.01 s	1.01 s	1.45 s	1.33 s
21	7.45 br s	7.43 br s	7.46 s	7.47 br s	7.47 br s	7.64 br s	7.49 br s
22	6.41 br d (1.2)	6.41 br d (0.8)	6.43 br d (0.8)	6.43 br d (1.2)	6.43 br d (0.8)	6.58 br d (1.2)	6.45 br d (1.2)
23	7.43 t (1.6)	7.42 t (1.6)	7.43 t (1.6)	7.42 t (1.6)	7.42 t (1.6)	7.60 t (1.6)	7.44 t (1.6)
28	1.19 s	1.20 s	1.20 s	1.00 s	0.99 s	1.01 s	1.13 s
29 _{pro-R}	1.77 d (13.2)	1.80 d (12.8)	1.97 d (12.6)	1.99 d (12.8)	1.98 d (12.4)	2.21 d (11.2)	2.35 d (12.8)
29 _{pro-S}	2.43 d (13.2)	2.45 d (12.8)	2.31 d (12.6)	2.15 d (12.8)	2.15 d (12.4)	2.88 d (11.2)	2.70 d (12.4)
30			3.46 br s	3.44 br s	3.45 br s		
31	3.86 s	3.85 s	3.87 s	3.67 s	3.67 s	3.80 s	3.86 s
	3-Acyl	3-Acyl	3-Acyl	3-Acyl	3-Acyl	3-Acyl	2-Acyl
33	2.15 s	2.57 m	2.13 s	2.66 m	2.47 m	1.94 s	2.42 m
	30-Acyl						
34	3.50 m	1.20 d (7.2)		1.21 d (6.8)	1.73 m	1-Acyl	1.48 m
	3.69 m				1.52 m		1.73 m
35	1.27 t (6.8)	1.22 d (7.2)		1.19 d (7.2)	0.94 t (7.2)	2.55 m	0.97 t (7.6)
		30-Acyl					
36		3.51 m			1.17 d (7.2)	1.11 d (7.2)	1.22 d (7.2)
		3.67 m					
37		1.27 t (6.8)			5.08 s	1.10 d (7.2)	
1-OH	2.91 br s	2.85 s					2.74 s
6-OH	2.92 d (3.2)	2.88 d (3.2)	2.94 br d (2.7)		5.58 d (4.8)	4.69 br d (3.6)	3.19 s
8-OH					5.05 s	5.00 s	
30-OH						4.87 s	3.43 s

¹ Recorded in CDCl₃; ² Recorded in acetone-*d*₆; ³ Overlapped signals assigned by ¹H-¹H COSY, HSQC, and HMBC spectra without designating multiplicity.

The relative configuration of **15** was assigned by analysis of NOE interactions (Figure 5b). Those between H-17/H-12 β , H-17/H-15 β , H-17/H-11 β , and H-11 β /H-5 revealed their cofacial relationship and were assigned as β -oriented. In turn, NOE interactions between H₃-18/H-15 α , H-9/H₃-19, H₃-19/1-OH, and H-34/H_{pro-R}-29 indicated the α -orientation for H-9, H₃-18, H₃-19, 1-OH, and 30-OEt. The NOE interaction between H-3/H_{pro-R}-29 established the 3 α -H and the corresponding 3 β -acetoxy function. Therefore, the relative configuration of **15** was determined. Comparison of the electronic circular dichroism (ECD) spectrum of **15** with that of thaixylomolin L [18] showed that **15** had the same 1*R*,3*S*,4*R*,5*S*,9*R*,10*S*,13*R*,17*R*,30*S*-absolute configuration as that of thaixylomolin L (Figure 6a). Thus, the structure of **15**—named xylomolin G₁—was assigned as depicted.

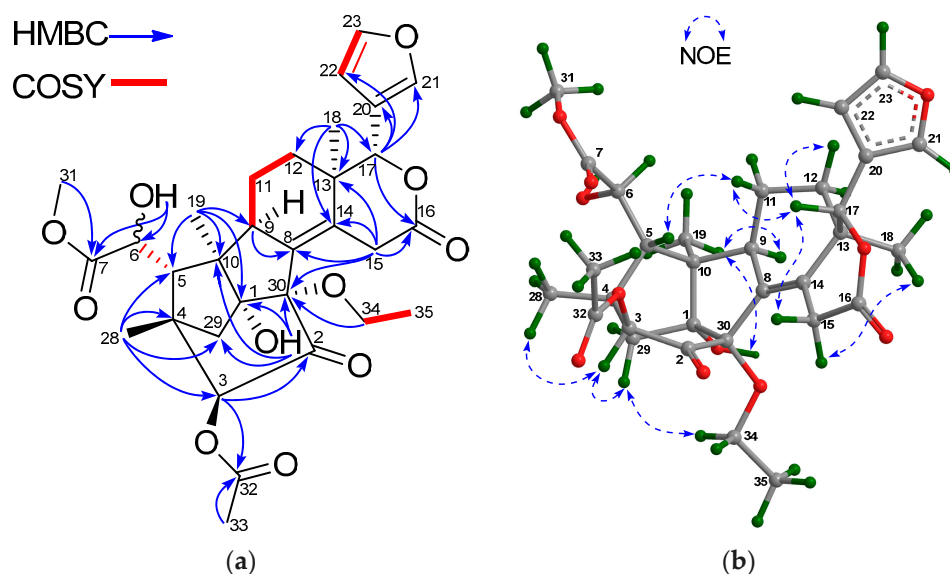


Figure 5. (a) Selected ^1H - ^1H COSY and HMBC correlations for compound **15** (measured in CDCl_3); (b) Diagnostic NOE interactions for compound **15** (measured in CDCl_3 , MM2-optimized structure).

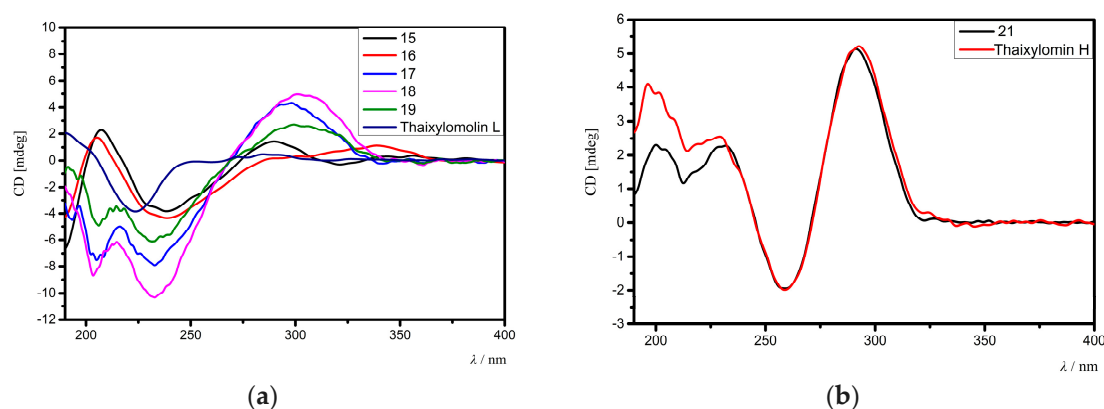


Figure 6. (a) Comparison of the experimental electronic circular dichroism (ECD) spectra of compounds **15**–**19** with that of the known compound, thaixylomolin L, containing a $\Delta^{8,14}$ double bonds; (b) Comparison of the experimental ECD spectra of compound **21** with that of the known compound, thaixylomolin H, containing $\Delta^{8,9}$, $\Delta^{14,15}$ conjugated double bonds.

Table 6. ^{13}C NMR spectroscopic data (100 MHz) of compounds **15–21** (δ in ppm).

Position	15 ¹	16 ¹	17 ¹	18 ¹	19 ²	20 ¹	21 ¹
1	84.5 qC	84.3 qC	85.2 qC	84.8 qC	84.8 qC	92.6 qC	85.5 qC
2	204.3 qC	204.1 qC	204.3 qC	204.1 qC	203.9 qC	209.1 qC	82.4 CH
3	84.8 CH	84.7 CH	85.0 CH	83.3 CH	83.0 CH	90.6 CH	207.8 qC
4	40.6 qC	40.6 qC	41.2 qC	40.6 qC	40.5 qC	45.1 qC	52.8 qC
5	45.4 CH	45.5 CH	46.0 CH	40.7 CH	40.5 CH	43.4 CH	51.4 CH
6	72.0 CH	72.1 CH	71.9 CH	34.2 CH ₂	34.2 CH ₂	71.9 CH	71.0 CH
7	175.3 qC	175.3 qC	175.4 qC	172.7 qC	172.7 qC	176.2 qC	175.2 qC
8	134.9 qC	135.0 qC	135.2 qC	134.5 qC	134.4 qC	76.8 qC	130.4 qC
9	48.3 CH	48.1 CH	49.4 CH	47.9 CH	48.0 CH	48.4 CH	156.6 qC
10	55.9 qC	56.0 qC	57.0 qC	56.4 qC	56.4 qC	48.0 qC	58.8 qC
11	19.5 CH ₂	19.5 CH ₂	20.2 CH ₂	19.4 CH ₂	19.4 CH ₂	17.8 CH ₂	20.2 CH ₂
12	31.9 CH ₂	32.0 CH ₂	32.2 CH ₂	31.9 CH ₂	31.9 CH ₂	29.5 CH ₂	30.0 CH ₂
13	40.7 qC	40.7 qC	40.4 qC	40.5 qC	40.6 qC	38.7 qC	37.8 qC
14	138.4 qC	138.5 qC	132.5 qC	133.0 qC	133.0 qC	160.0 qC	154.9 qC
15	33.1 CH ₂	33.0 CH ₂	35.4 CH ₂	35.4 CH ₂	35.3 CH ₂	120.2 CH	113.4 CH
16	169.6 qC	169.9 qC	169.8 qC	170.3 qC	170.3 qC	164.9 qC	165.7 qC
17	80.5 CH	80.5 CH	80.8 CH	80.7 CH	80.7 CH	81.2 CH	80.4 CH
18	17.7 CH ₃	17.4 CH ₃	17.5 CH ₃	16.8 CH ₃	16.8 CH ₃	21.4 CH ₃	16.2 CH ₃
19	17.0 CH ₃	17.1 CH ₃	16.7 CH ₃	14.9 CH ₃	14.9 CH ₃	22.2 CH ₃	15.7 CH ₃
20	120.6 qC	120.6 qC	120.6 qC	120.5 qC	120.5 qC	121.1 qC	120.3 qC
21	141.1 CH	141.1 CH	141.1 CH	141.2 CH	141.1 CH	142.7 CH	141.2 CH
22	110.0 CH	110.0 CH	110.1 CH	110.1 CH	110.1 CH	111.1 CH	110.1 CH
23	143.1 CH	143.1 CH	143.0 CH	142.9 CH	142.9 CH	144.0 CH	143.0 CH
28	19.8 CH ₃	19.7 CH ₃	19.5 CH ₃	19.2 CH ₃	19.2 CH ₃	15.7 CH ₃	16.3 CH ₃
29	44.7 CH ₂	44.9 CH ₂	45.4 CH ₂	44.6 CH ₂	44.5 CH ₂	41.5 CH ₂	39.3 CH ₂
30	92.2 qC	92.3 qC	63.0 CH	63.4 CH	63.5 CH	83.6 qC	82.4 qC
31	53.2 CH ₃ 3-Acyl	53.1 CH ₃ 3-Acyl	53.3 CH ₃ 3-Acyl	51.8 CH ₃ 3-Acyl	51.7 CH ₃ 3-Acyl	53.0 CH ₃ 3-Acyl	53.3 CH ₃ 2-Acyl
32	169.9 qC	176.0 qC	170.1 qC	176.5 qC	176.0 qC	170.1 qC	176.0 qC
33	20.6 CH ₃	33.8 CH	20.7 CH ₃	33.9 CH	40.8 CH	21.3 CH ₃	41.3 CH
34	63.3 CH ₂	19.0 CH ₃		18.9 CH ₃	26.7 CH ₂	176.0 qC	26.5 CH ₂
35	15.7 CH ₃	19.1 CH ₃ 30-Acyl		18.9 CH ₃	11.5 CH ₃	35.1 CH	11.7 CH ₃
36		63.4 CH ₂		17.0 CH ₃	16.5 CH ₃	19.4 CH ₃	17.2 CH ₃
37		15.7 CH ₃				19.3 CH ₃	

¹ Recorded in CDCl₃; ² Recorded in acetone-*d*₆.

Compound **16** had a molecular formula of C₃₃H₄₂O₁₁ as determined from the positive HRESIMS ion peak at *m/z* 615.2809 (calcd. for [M + H]⁺, 615.2805). The NMR spectroscopic data of **16** (Tables 5 and 6) were closely related to those of **15**, the difference being the replacement of 3-acetoxy group in **15** by an isobutyryloxy group (δ_{H} 2.57 m, 1.20 d (*J* = 7.2 Hz), 1.22 d (*J* = 7.2 Hz); δ_{C} 176.0 qC, 33.8 CH, 19.0 CH₃, 19.1 CH₃) in **16**. The presence of the above isobutyryloxy group was further supported by ¹H-¹H COSY correlations between H₃-34/H-33 and H₃-35/H-33, and HMBC correlations between H-33/C-32, H₃-34/C-32, and H₃-35/C-32. The significant HMBC cross-peak from H-3 to the carbonyl carbon (C-32) of the isobutyryloxy group confirmed its location at C-3. NOE interactions between H-17/H-12 β , H-17/H-15 β , H-17/H-11 β , H-11 β /H-5, H-17/H-5, H-5/H₃-28, H-3/H_{pro-R}-29, H-15 α /H₃-18, H₃-18/H-9, H-9/H₃-19, and 1-OH/H-9 indicated the same relative configuration of **16** as that of **15**. Comparison of the ECD spectrum of **16** with that of thaixylomolin L concluded that **16** had the same 1*R*,3*S*,4*R*,5*S*,9*R*,10*S*,13*R*,17*R*,30*S*-absolute configuration as that of thaixylomolin L (Figure 6a). Thus, the structure of **16**—named xylomolin G₂—was assigned as 3-*O*-isobutyryl-3-deacetoxy-xylomolin G₁.

Compound **17** was isolated as an amorphous yellow solid. Its molecular formula was determined to be C₂₉H₃₄O₁₀ by the positive HRESIMS ion peak at *m/z* 543.2246 (calcd. for [M + H]⁺, 543.2230).

The similarities between the NMR spectroscopic data of **17** (Tables 5 and 6) and **15** revealed their close structural resemblance, except for the absence of the ethoxyl group at C-30, which was confirmed by the upshifted C-30 signal (δ_C 63.0 CH in **17**, whereas δ_C 92.2 qC in **15**) and HMBC cross-peaks between H-30/C-1, H-30/C-2, H-30/C-8, and H-30/C-10. The relative configuration of **17** was determined to be identical to that of **15** by analysis of NOE interactions. Comparison of ECD spectra of **17** and **15** concluded that both compounds had the same 1*R*,3*S*,4*R*,5*S*,9*R*,10*S*,13*R*,17*R*,30*S*-absolute configuration (Figure 6a). Thus, the structure of **17**—named xylomolin G₃—was assigned as 30-deethoxyl-xylomolin G₁.

Compound **18** provided the molecular formula C₃₁H₃₈O₉ as established by the positive HRESIMS ion peak at m/z 555.2593 (calcd. for [M + H]⁺, 555.2594). The NMR spectroscopic data of **18** (Tables 5 and 6) were similar to those of **15**, the difference being the absence of the 30-ethoxyl group and the 6-OH function in **18**. The upshifted C-30 (δ_C 63.4 CH in **18**, whereas δ_C 92.2 qC in **15**) and C-6 (δ_C 34.2 CH₂ in **18**, whereas δ_C 72.1 CH in **15**) signals and HMBC cross-peaks between H-30/C-1, H-30/C-2, H-30/C-8, H-30/C-10, H-6/C-5, and H-6/C-7 supported the above deduction. The relative and absolute configurations of **18** were determined to be the same as that of **15** by analysis of their NOE interactions and ECD spectra (Figure 6a). Thus, the structure of **18**—named xylomolin G₄—was concluded to be 30-deethoxyl-6-dehydroxy-xylomolin G₁.

Compound **19** gave the molecular formula C₃₂H₄₀O₉ as determined from the positive HRESIMS ion peak at m/z 569.2753 (calcd. for [M + H]⁺, 569.2751). The NMR data of **19** (Tables 5 and 6) were closely related to those of **18**, except for the replacement of the 3-isobutyryloxy group in **18** by a 2-methylbutyryloxy group (δ_H 2.47 m 1H, 1.73 m 1H, 1.52 m 1H, 0.94 t ($J = 7.2$ Hz 3H), 1.19 d ($J = 7.2$ Hz 3H); δ_C 176.0 qC, 40.8 CH, 26.7 CH₂, 11.5 CH₃, 16.5 CH₃) in **19**. The presence of the 2-methylbutyryloxy group was supported by the ¹H-¹H COSY correlations between H-33/H-34, H-33/H₃-36, and H-34/H₃-35 and HMBC cross-peaks between H-33/C-32, H₂-34/C-32, H₃-36/C-32, H₃-36/C-34, and H₃-35/C-33. The significant HMBC cross-peak from H-3 to the carbonyl carbon (C-32) of the above 2-methylbutyryloxy group assigned its location at C-3. The relative and absolute configurations of **19** were determined to be the same as those of **18** by analysis of their NOE interactions and ECD spectra (Figure 6a). Thus, the structure of **19**—named xylomolin G₅—was assigned as 3-*O*-(2-methyl)butyryl-3-deisobutyryloxy-xylomolin G₄.

Compound **20** was isolated as an amorphous white powder. Its molecular formula was determined to be C₃₃H₄₀O₁₃ by the positive HRESIMS ion peak at m/z 667.2359 (calcd. for [M + Na]⁺, 667.2361). The NMR spectroscopic data of **20** (Tables 5 and 6) resembled those of **15**, except for the presence of an additional 8-OH group (δ_H 5.00 s) and the replacement of the $\Delta^{8,14}$ double bond, 1-OH function, and 30-ethoxyl group in **15** by a $\Delta^{14,15}$ double bond (δ_H 5.72 br s H-15; δ_C 160.0 qC C-14, 120.2 CH C-15), a 1-*O*-isobutyryl moiety (δ_H 2.55 m H-35, 1.11 d ($J = 7.2$ Hz H₃-36), 1.10 d ($J = 7.2$ Hz H₃-37); δ_C 176.0 qC C-34, 35.1 CH C-35, 19.4 CH₃ C-36, 19.3 CH₃ C-37), and a 30-OH group (δ_H 4.87 s) in **20**, respectively (Tables 5 and 6, recorded in CDCl₃). HMBC correlations between H-15/C-14, H-15/C-16, H-15/C-13, H-15/C-8, 8-OH/C-8, and 30-OH/C-30 confirmed the presence of a $\Delta^{14,15}$ double bond and the existence of two hydroxy groups at C-8 and C-30, respectively. The presence of the isobutyryloxy group was supported by ¹H-¹H COSY cross-peaks between H-35/H₃-36 and H-35/H₃-37 and HMBC correlations between H-35/C-34, H₃-36/C-34, and H₃-37/C-34. Its location at C-1 was corroborated by the downshifted C-1 signal (δ_C 92.6 qC in **20**, whereas δ_C 84.5 qC in **15**). The relative configuration of **20** was established by NOE interactions, in which those between H-17/H-12 β , H-12 β /H-5, H-5/H₃-28 assigned the β -orientation for H-17, H-5, H₃-28, whereas those between H-11 α /H₃-18, H₃-18/8-OH, 8-OH/H-9, H_{pro-R}-29/H-3, H-9/H₃-19, and H-3/30-OH concluded the α -orientation for H₃-18, 8-OH, H-9, H-3, H₃-19, and 30-OH. Thus, the structure of **20**—named xylomolin H—was assigned as depicted.

Compound **21** afforded the molecular formula C₃₂H₃₈O₁₁ as deduced from the positive HRESIMS ion peak at m/z 621.2304 (calcd. for [M + Na]⁺, 621.2306). The NMR spectroscopic data of **21** (Tables 5 and 6) were similar to those of thaixylomolin H [18], except for the presence of an additional 6-OH group (δ_H 3.19 s) and the replacement of the 2-acetoxy group by a 2-methylbutyryloxy moiety (δ_H 2.42 m 1H, 1.73 m 1H, 1.48 m 1H, 0.97 t ($J = 7.6$ Hz 3H), 1.22 d ($J = 7.2$ Hz

3H); δ_C 176.0 qC, 41.3 CH, 26.5 CH₂, 11.7 CH₃, 17.2 CH₃) in **21**. The presence of the 6-OH group was supported by the downshifted C-6 signal (δ_C 71.0 CH in **21**, whereas δ_C 31.6 CH₂ in thaixylomolin H), the ¹H-¹H COSY cross-peak between H-5/H-6, and HMBC correlations between H-6/C-5 and H-6/C-7. The existence of the 2-methylbutyryloxy group was corroborated by ¹H-¹H COSY cross-peaks between H-33/H₃-36, H-33/H-34, and H₂-34/H₃-35 and HMBC correlations between H-33/C-32, H-34/C-32, H₃-36/C-32, H-33/C-34, H₃-36/C-34, H₃-35/C-34, H-34/C-33, H₃-35/C-33, and H₃-36/C-33. The significant HMBC correlation from H-2 to the carbonyl carbon (C-32) of the 2-methylbutyryloxy group placed it at C-2. NOE interactions between H-17/H-12 β , H-11 α /H₃-19, H-11 α /H₃-18, H-11 β /H-5, H-5/H₃-28, H₃-19/1-OH, H_{pro-R}-29/H-2, and H-2/30-OH assigned the β -orientation for H-17, H₃-28, and H-5, and the α -orientation for H-2, H₃-18, H₃-19, 30-OH, and 1-OH. The ECD spectrum of **21** was identical to that of thaixylomolin H (Figure 6b), concluding that **21** had the same 1*R*,2*R*,4*R*,5*R*,10*S*,13*R*,17*R*,30*R*-absolute configuration as that of thaixylomolin H. Thus, the structure of **21**—named xylomolin I—was identified as 6-hydroxy-2-*O*-(2-methyl)butyryl-2-deacetoxy-thaixylomolin H.

Compound **22** had the molecular formula C₂₉H₃₂O₁₀ as determined from the positive HRESIMS ion peak at *m/z* 541.2077 (calcd. for [M + H]⁺, 541.2074). The similarities between the NMR spectroscopic data of **22** (Tables 7 and 8) and those of trangmolin F [16], containing a (*Z*)-bicyclo[5.2.1]dec-3-en-8-one substructure, revealed their close structural resemblance. However, the 3-*O*-isobutyryl function in trangmolin F was replaced by an acetoxy group (δ_H 2.17 s 3H; δ_C 170.4 qC, 20.6 CH₃) in **22**, being unambiguously confirmed by HMBC cross-peaks between H-3/C-32 and H₃-33/C-32 (Figure 7a). The relative configuration of **22** was assigned by NOE interactions (Figure 7b). Those between H-17/H-12 β , H-12 β /H₃-19, and H₃-19/H-5 revealed their cofacial relationship and were determined as β -oriented, whereas those between H-3/H-9, H_{pro-R}-29/H-3, and H-12 α /H₃-18 indicated the α -orientation for H-3, H-9, and H₃-18, and the corresponding 3 β -acetoxy function. The ECD spectrum of **22** was nicely matched with that of trangmolin F (Figure 8a), concluding that the absolute configuration of **22** was the same as that of trangmolin F. Thus, the structure of **22**—named xylomolin J₁—was assigned as 3-*O*-acetyl-3-deisobutyryloxy-trangmolin F.

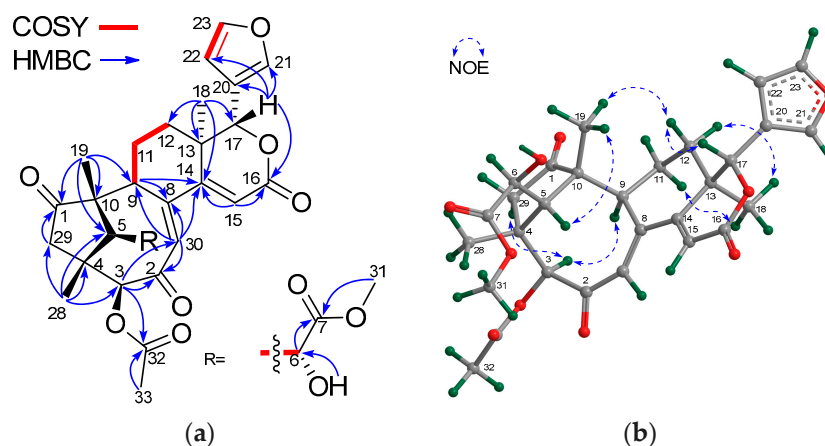


Figure 7. (a) Selected ¹H-¹H COSY and HMBC correlations for compound **22** (measured in CDCl₃); (b) Diagnostic NOE interactions for compound **22** (measured in CDCl₃, MM2-optimized structure).

Table 7. ¹H NMR spectroscopic data (400 MHz, in CDCl₃) of compounds 22–29 (δ in ppm, *J* in Hz).

Position	22	23	24	25	26	27	28	29
1							7.14 d (10.4)	3.52 m
2β							5.90 d (10.4)	2.92 dd (14.4,6.4)
2α								2.46 dd (14.4,3.6)
3	5.54 s	5.50 s	4.88 s	4.86 s	5.17 s	4.82 s		
5	2.92 s	2.94 s	2.80 br s	2.82 s	2.40 s	2.37 d (13.6)	2.22 dd (12.4, 2.8)	2.82 d (10.4)
6a	4.26 br s	4.27 br s	4.58 s	4.58 s	4.51 s	2.40 br d (23.2)	1.93 m (α)	2.24 d (16.4)
6b						2.42 dd (23.2, 13.6)	1.99 m (β)	2.62 dd (16.4, 10.4)
7							5.30 t (2.8)	
9	3.23 m	3.25 m					2.54 m	2.22 m
11α	1.89 m	1.88 m	2.63 m	2.62 m	1.94 m	1.98 t (14.4)	2.10 m	1.65 m
11β	1.75 m	1.74 m	2.37 m	2.37 dd (20.0, 3.6)	2.26 m	2.19 dd (14.4, 4.0)	1.83 m	2.30 m
12β	1.83 m	1.83 m	1.39 m	1.40 td (12.8, 4.8)	1.56 m	3.87 br d (13.6)	1.70 m	1.96 m
12α	1.25 m	1.24 m	1.72 m	1.72 dd (12.8, 4.0)	1.25 m		2.20 m	1.35 dd (17.2, 4.4)
15α	6.00 s	5.99 s	7.23 s	7.18 s	6.56 s	6.00 s	5.87 s	2.86 d (18.0)
15β								2.60 d (18.0)
17	5.33 s	5.34 s	5.01 s	5.01 s	5.61 s	5.80 s	2.53 overlapped	5.66 s
18	1.08 s	1.07 s	1.04 s	1.04 s	1.38 s	1.43 s	1.43 s	0.93 s
19	1.21 s	1.22 s	1.54 s	1.54 s	1.54 s	1.33 s	1.24 s	0.97 s
20							2.97 ddd (12.0, 9.2, 2.8)	
21α	7.53 br s	7.53 br s	7.51 br s	7.51 s	7.45 br s	7.67 br s		4.85 br d (18.3)
21β								5.03 dd (18.3, 2.0)
22α	6.49 d (1.2)	6.49 d (1.2)	6.48 br d (1.2)	6.47 br d (1.2)	6.41 br s	6.61 br s	2.44 m	6.08 br s
22β							2.49 m	
23α	7.47 t (1.6)	7.47 t (1.6)	7.46 t (1.6)	7.45 t (1.6)	7.43 br s	7.53 br s	4.23 ddd (10.4, 9.2, 6.8)	
23β							4.46 td (8.8, 2.0)	
28	1.21 s	1.22 s	1.00 s	1.00 s	0.87 s	0.82 s	1.10 s	1.03 s

Table 7. Cont.

Position	22	23	24	25	26	27	28	29
29 _{pro-R}	2.49 d (19.2)	2.46 br d (18.8)	1.81 dd (10.8, 2.0)	1.81 dd (10.4, 2.0)	1.67 br d (11.0)	1.80 d (11.2)	1.09 s	1.20 s
29 _{pro-S}	2.56 d (19.2)	2.58 d (18.8)	2.71 d (10.8)	2.70 d (10.4)	2.36 d (11.0)	1.86 d (11.2)		
30 α	6.59 br d (1.6)	6.56 br d (1.6)			5.34 s	4.49 s	1.29 s	4.92 s (30a)
30 β								5.22 s (30b)
31	3.81 s	3.81 s	3.81 s	3.82 s	3.80 s	3.76 s	7-Acyl	3.73 s
32	3-Acyl	3-Acyl	3-Acyl	3-Acyl			1.97 s	
33	2.17 s	2.51 m	2.27 m	2.45 m	1.70 s	1.68 s		
34		1.53 m	1.42 m		3-Acyl	3-Acyl		
		1.74 m	1.58 m					
35		0.96 t (7.2)	0.87 t (7.6)	1.11 d (6.8)	2.07 s			
36		1.18 d (7.2)	1.07 d (6.8)	1.11 d (6.8)	2-Acyl	6.88 q (6.8)		
37					2.17 s	1.73 br d (6.8)		
38						1.84 s		
1-OH			2.81 s	2.84 br s		3.45 s		
2-OH			4.93 s	4.93 br s		3.57 s		
6-OH	3.01 s	3.06 br s	3.12 br s	3.13 s				

Table 8. ¹³C NMR spectroscopic data (100 MHz, in CDCl₃) of compounds 22–29 (δ in ppm).

Position	22	23	24	25	26	27	28	29
1	215.1 qC	215.4 qC	85.8 qC	85.9 qC	84.4 qC	84.4 qC	156.7 CH	77.5 CH
2	193.6 qC	193.5 qC	80.7 qC	80.8 qC	84.0 qC	75.7 qC	126.0 CH	39.2 CH ₂
3	82.9 CH	82.4 CH	87.2 CH	87.2 CH	85.6 CH	86.6 CH	204.0 qC	212.4 qC
4	41.1 qC	41.2 qC	45.6 qC	45.6 qC	44.4 qC	43.7 qC	44.1 qC	48.1 qC
5	49.2 CH	49.2 CH	48.2 CH	48.1 CH	44.8 CH	40.5 CH	46.2 CH	42.9 CH
6	70.9 CH	70.9 CH	71.5 CH	71.5 CH	71.5 CH	33.8 CH ₂	23.5 CH ₂	32.6 CH ₂
7	175.1 qC	175.2 qC	175.0 qC	174.9 qC	174.1 qC	174.1 qC	73.9 CH	173.7 qC
8	149.7 qC	149.6 qC	121.0 qC	121.1 qC	84.0 qC	83.7 qC	44.8 qC	144.8 qC
9	43.7 CH	44.1 CH	169.8 qC	169.7 qC	86.8 qC	87.1 qC	37.8 CH	49.6 CH
10	52.7 qC	52.6 qC	48.8 qC	48.8 qC	49.0 qC	47.4 qC	39.9 qC	44.0 qC

Table 8. Cont.

Position	22	23	24	25	26	27	28	29
11	21.0 CH ₂	21.2 CH ₂	25.6 CH ₂	25.6 CH ₂	26.3 CH ₂	34.3 CH ₂	15.8 CH ₂	23.7 CH ₂
12	30.8 CH ₂	30.8 CH ₂	30.1 CH ₂	30.1 CH ₂	29.5 CH ₂	66.5 CH	31.5 CH ₂	29.2 CH ₂
13	40.0 qC	40.0 qC	36.5 qC	36.5 qC	38.1 qC	44.7 qC	47.9 qC	41.8 qC
14	165.9 qC	166.2 qC	152.1 qC	152.2 qC	154.6 qC	152.3 qC	193.6 qC	80.1 qC
15	115.1 CH	115.0 CH	115.8 CH	115.7 CH	122.3 CH	123.7 CH	123.8 CH	33.5 CH ₂
16	163.8 qC	163.8 qC	165.4 qC	165.5 qC	163.9 qC	162.4 qC	205.1 qC	168.2 qC
17	79.2 CH	79.1 CH	80.3 CH	80.3 CH	80.6 CH	78.2 qC	61.8 CH	81.2 CH
18	19.6 CH ₃	19.6 CH ₃	15.8 CH ₃	15.8 CH ₃	19.6 CH ₃	13.2 CH ₃	24.2 CH ₃	14.1 CH ₃
19	15.3 CH ₃	15.4 CH ₃	16.1 CH ₃	16.0 CH ₃	17.4 CH ₃	15.6 CH ₃	19.1 CH ₃	21.7 CH ₃
20	119.6 qC	119.7 qC	119.9 qC	119.9 qC	119.6 qC	121.5 qC	36.8 CH	164.3 qC
21	141.5 CH	141.5 CH	141.3 qC	141.3 CH	141.5 CH	142.3 CH	177.5 qC	72.4 CH ₂
22	110.0 CH	110.1 CH	110.0 CH	110.0 CH	109.8 CH	109.7 CH	29.2 CH ₂	117.8 CH
23	143.4 CH	143.4 CH	143.2 CH	143.2 CH	143.2 CH	144.9 CH	66.5 CH ₂	172.5 qC
28	16.7 CH ₃	16.5 CH ₃	16.6 CH ₃	16.6 CH ₃	15.4 CH ₃	14.5 CH ₃	27.0 CH ₃	25.5 CH ₃
29	49.7 CH ₂	49.6 CH ₂	43.1 CH ₂	43.1 CH ₂	40.5 CH ₃	39.0 CH ₃	21.3 CH ₃	21.4 CH ₃
30	134.7 CH	134.8 CH	194.9 qC	195.0 qC	74.0 CH	78.2 CH	26.8 CH ₃	112.5 CH ₂
31	53.2 CH ₃	53.2 CH ₃	53.3 CH ₃	53.3 CH ₃	53.2 CH ₃	52.3 CH ₃	169.8 qC	52.2 CH ₃
32	3-Acyl	3-Acyl	3-Acyl	3-Acyl	119.5 qC	119.4 qC	21.0 CH ₃	
33	170.4 qC	176.2 qC	174.3 qC	174.8 qC	16.6 CH ₃	16.5 CH ₃		
34		26.6 CH ₂	26.5 CH ₂	18.8 CH ₃	169.0 qC	167.8 qC		
35		11.5 CH ₃	11.8 CH ₃	19.0 CH ₃	21.7 CH ₃	130.1 qC		
36		16.4 CH ₃	16.7 CH ₃		2-Acyl	170.7 qC	139.7 CH	
37					21.9 CH ₃	14.4 CH ₃		
38						12.5 CH ₃		

Compound **23** provided the molecular formula of $C_{32}H_{38}O_{10}$ as established by the positive HRESIMS ion peak at m/z 583.2548 (calcd. for $[M + H]^+$, 583.2543). The NMR spectroscopic data of **23** (Tables 7 and 8) resembled those of **22**, except for the replacement of the 3-acetoxy group in **22** by a 2-methylbutyryloxy moiety (δ_H 2.51 m 1H, 1.53 m 1H, 1.74 m 1H, 0.96 t ($J = 7.2$ Hz, 3H), 1.18 d ($J = 7.2$ Hz, 3H); δ_C 176.2 qC, 40.7 CH, 26.6 CH_2 , 11.5 CH_3 , 16.4 CH_3) in **23**. The presence of the 2-methylbutyryloxy group was further evidenced by 1H - 1H COSY cross-peaks between H-33/ H_3 -36, H-33/ H_2 -34, and H_2 -34/ H_3 -35 and HMBC correlations between H-33/C-32, H-34/C-32, and H_3 -36/C-32. The HMBC correlation from H-3 to the carbonyl carbon (C-32) of the above 2-methylbutyryloxy group placed it at C-3. The relative configuration of **23** was confirmed to be the same as that of **22** by analysis of NOE interactions. Comparison of ECD spectra of compounds **23**, **22**, and trangmolin F (Figure 8a) revealed that these compounds had the same absolute configuration. The absolute configuration of C-6 was further determined by the modified Mosher α -methoxy- α -(trifluoromethyl)phenylacetyl (MTPA) ester method [24]. The $\Delta\delta$ values of H-5, H_3 -19, and H_3 -29 were positive, while that of H_3 -31 was negative (Figure 8b). This regular arrangement concluded the *R*-absolute configuration for C-6. Finally, the absolute configuration of **23**—named xylomolin J_2 —was unequivocally established as 3*S*,4*R*,5*S*,6*R*,9*S*,10*R*,13*R*,17*R*.

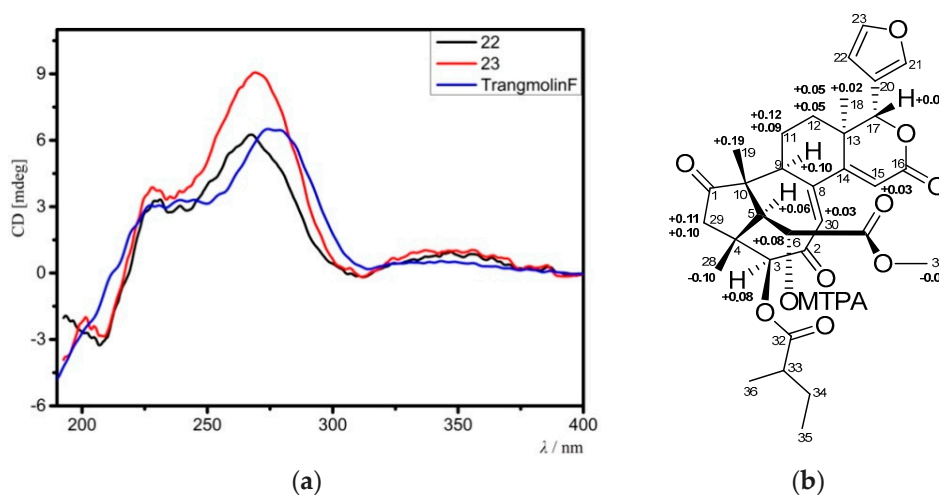


Figure 8. (a) Comparison of the experimental ECD spectra of compounds **22**, **23** with that of the known compound, trangmolin F; (b) $\Delta\delta$ values ($\Delta\delta$ [ppm] = $[\delta_S - \delta_R]$) obtained for the (6*S*) and (6*R*)-MTPA esters of **23**. MTPA: α -methoxy- α -(trifluoromethyl)phenylacetyl.

Compound **24** had the molecular formula $C_{32}H_{38}O_{11}$ as determined from the positive HRESIMS ion peak at m/z 621.2306 (calcd. for $[M + Na]^+$, 621.2306). The NMR spectroscopic data of **24** (Tables 7 and 8) were similar to those of moluccensin I [25], except for the presence of an additional 6-OH group (δ_H 3.12 br s) and the replacement of the 1-*O*-isobutyryl group in moluccensin I by a 1-OH function (δ_H 2.81 s) in **24**. The downshifted C-6 signal (δ_C 71.5 CH in **24**, whereas δ_C 33.2 CH_2 in moluccensin I) and HMBC correlations from the active proton (δ_H 3.12 br s) to C-5, C-6, and C-7 revealed the presence of the 6-OH group (Figure 9a). The existence of the 1-OH function was confirmed by the upshifted C-1 signal (δ_C 85.8 qC in **24**, whereas δ_C 90.8 qC in moluccensin I) and strong HMBC cross-peaks from the active proton (δ_H 2.81 s) to C-1, C-2, and C-10 (Figure 9a). The relative configuration of **24** was identified as the same as that of moluccensin I based on NOE interactions between H-17/H-12 β , H-5/H-11 β , H-5/H-28, H_3 -18/H-11 α , H_3 -19/ H_{pro-S} -29, H-3/ H_{pro-R} -29, and 2-OH/ H_{pro-R} -29 (Figure 9b). Therefore, the structure of **24**—named xylomolin K_1 —was assigned as 6-hydroxy-1-*O*-deisobutyryl-moluccensin I.

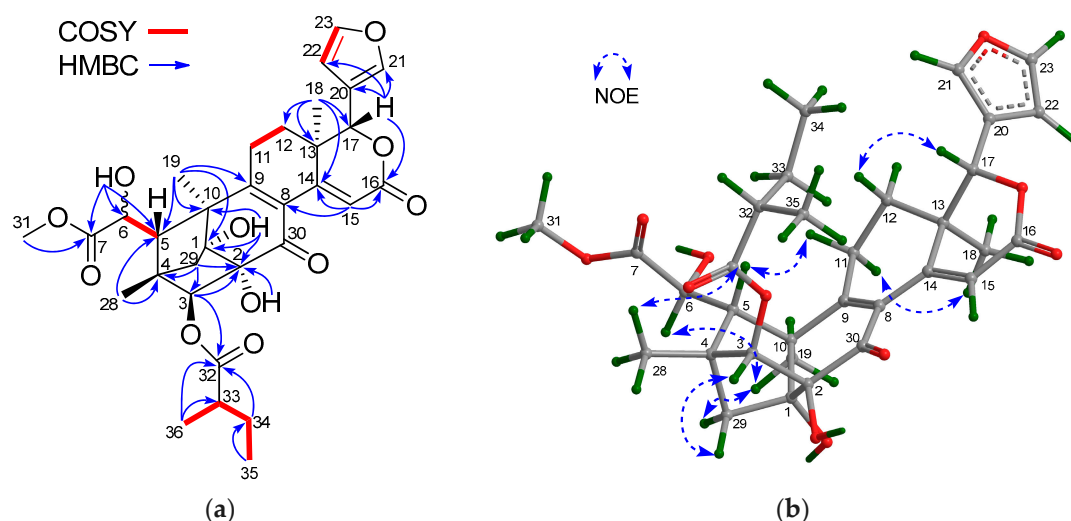


Figure 9. (a) Selected ^1H - ^1H COSY and HMBC correlations for compound **24** (measured in CDCl_3); (b) Diagnostic NOE interactions for compound **24** (measured in CDCl_3 , MM2-optimized structure).

Compound **25** provided the molecular formula $\text{C}_{31}\text{H}_{36}\text{O}_{11}$ as determined from the positive HRESIMS ion peak at m/z 607.2164 (calcd. for $[\text{M} + \text{Na}]^+$, 607.2150). The NMR spectroscopic data of **25** (Tables 7 and 8) were similar to those of **24**, except for the replacement of 3-*O*-(2-methyl)butyryl in **24** by an isobutyryloxy group (δ_{H} 2.45 m 1H, 1.11 d ($J = 6.8$ Hz, 3H), 1.11 d ($J = 6.8$ Hz, 3H); δ_{C} 174.8 qC, 34.2 CH, 18.8 CH_3 , 19.0 CH_3) in **25**. The HMBC correlation from H-3 to the carbonyl carbon (C-32) of the isobutyryloxy group placed it at C-3. The relative configuration of **25** was determined to be the same as that of **24** based on NOE interactions between H-17/H-12 β , H-11 β /H-5, H-5/H₃-28, H-12 α /H₃-18, H₃-18/H-11 α , H_{pro-R}-29/H-3, and H_{pro-S}-29/H₃-19. Thus, the structure of **25**—named xylomolin K₂—was identified as 3-*O*-isobutyryl-3-de(2-methyl)butyryloxy-xylomolin K₁.

Compound **26** was obtained as an amorphous white powder. Its molecular formula was determined to be $\text{C}_{33}\text{H}_{38}\text{O}_{14}$ by the positive HRESIMS ion peak at m/z 681.2149 (calcd. for $[\text{M} + \text{Na}]^+$, 681.2154). The NMR spectroscopic data of **26** (Tables 7 and 8) resembled those of 2-*O*-acetyl-2-dehydroxy-12-deacetylxyloccensin U [18], being a phragmalin 8,9,30-*ortho* ester isolated from *X. moluccensis*, except for the presence of an additional 6-OH group and the absence of the 12-OH group in **26**. The presence of the 6-OH group was supported by the downshifted C-6 signal (δ_{C} 71.5 CH in **26**, whereas δ_{C} 33.7 CH_2 in 2-*O*-acetyl-2-dehydroxy-12-deacetylxyloccensin U), the ^1H - ^1H COSY cross-peak between H-5/H-6 and HMBC correlations between H-6/C-5 and H-6/C-7. The upshifted C-12 signal (δ_{C} 29.5, CH_2 in **26**, whereas δ_{C} 66.6 CH in 2-*O*-acetyl-2-dehydroxy-12-deacetylxyloccensin U), ^1H - ^1H COSY cross-peaks between H₂-11/H₂-12, and HMBC correlations between H₃-18/C-12 (Figure 10a) confirmed the absence of the 12-OH group in **26**. NOE correlations between H-17/H-12 β , H-12 β /H-5, H-17/H-5, H-5/H-30, H₃-18/H-12 α , H₃-18/H-11 α , H₃-19/H_{pro-S}-29, and H-3/H_{pro-R}-29 revealed the same relative configuration of **26** as that of 2-*O*-acetyl-2-dehydroxy-12-deacetylxyloccensin U (Figure 10b). The ECD spectrum of **26** was nicely matched with that of 2-*O*-acetyl-2-dehydroxy-12-deacetylxyloccensin U (Figure 10c), revealing the same absolute configuration for the two compounds. Thus, the structure of **26**—named xylomolin L₁—was assigned as 6-hydroxy-12-dehydroxy-2-*O*-acetyl-2-dehydroxy-12-deacetylxyloccensin U.

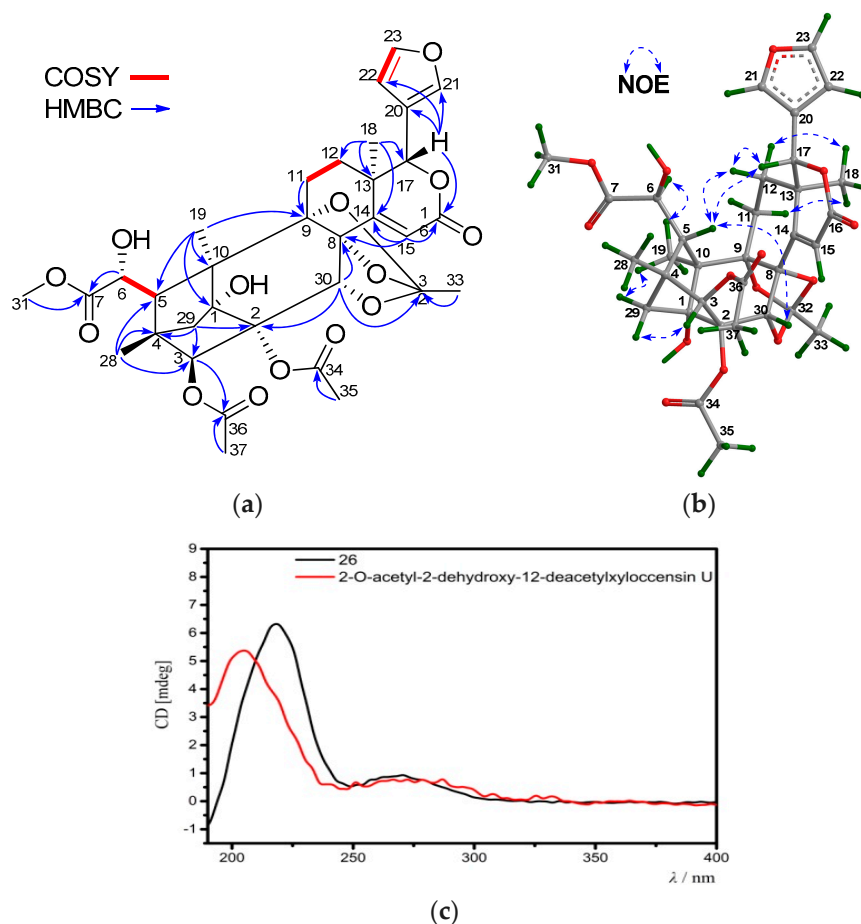


Figure 10. (a) Selected ^1H - ^1H COSY and HMBC correlations for compound **26** (measured in CDCl_3); (b) Diagnostic NOE interactions for compound **26** (measured in CDCl_3 , MM2-optimized structure); (c) Comparison of the experimental ECD spectrum of compound **26** with that of the known compound, 2-O-acetyl-2-dehydroxy-12-deacetylxyloccensin U.

The molecular formula of **27** was determined to be $\text{C}_{34}\text{H}_{40}\text{O}_{13}$ by the positive HRESIMS ion peak at m/z 679.2374 (calcd. for $[\text{M} + \text{Na}]^+$, 679.2361). The NMR spectroscopic data of **27** (Tables 7 and 8) closely resembled those of swietephragmin G [26], being a phragmalin 8,9,30-*ortho* ester, except for the presence of an additional 12-OH group, which was supported by the downshifted C-12 signal (δ_{C} 66.5 CH in **27**, whereas δ_{C} 29.2 CH_2 in swietephragmin G), ^1H - ^1H COSY cross-peaks between H_2 -11/ H -12, and HMBC correlations between H_3 -18/C-12. The strong NOE interaction between H -17/ H -12 assigned the β -oriented H -12 and the corresponding α -orientation for the 12-OH group. The NOE interaction between H_3 -37/ H_3 -38 assigned the *E* configuration for the double bond of 3-tigloyloxy group. Therefore, the structure of **27**—named xylomolin L₂—was identified as 12 α -hydroxy-swietephragmin G.

Compound **28** had the molecular formula $\text{C}_{28}\text{H}_{37}\text{O}_6$ as determined from the positive HRESIMS ion peak at m/z 469.2603 (calcd. for $[\text{M} + \text{H}]^+$, 469.2585). The NMR spectroscopic data of **28** (Tables 7 and 8) were closely related to those of andirolide Q [27], except for the different positions of the ester carbonyl carbon of the C-17 attached five-membered γ -lactone ring, *viz.* C-21 in **28** instead of C-23 in andirolide Q. Significant ^1H - ^1H COSY correlations between H -17/ H -20, H -20/ H_2 -22, H_2 -22/ H_2 -23 and the HMBC correlation between H -17/C-21 confirmed the above deduction (Figure 11a). NOE interactions between H -17/ H -12 β , H -12 β / H_3 -30, H_3 -30/ H -7, H_3 -30/ H -11 β , H -11 β / H_3 -19, and H_3 -18/ H -11 α , H_3 -18/ H -12 α , H_3 -18/ H -20, H_3 -18/ H -9, and H -9/ H -5 indicated the β -orientation for H -7, H -17, H_3 -19,

and H₃-30, and the α -orientation for H-5, H-9, H₃-18, and H-20 (Figure 11b). Hence, the relative configuration of **28**—named xylomolin M—was assigned as depicted.

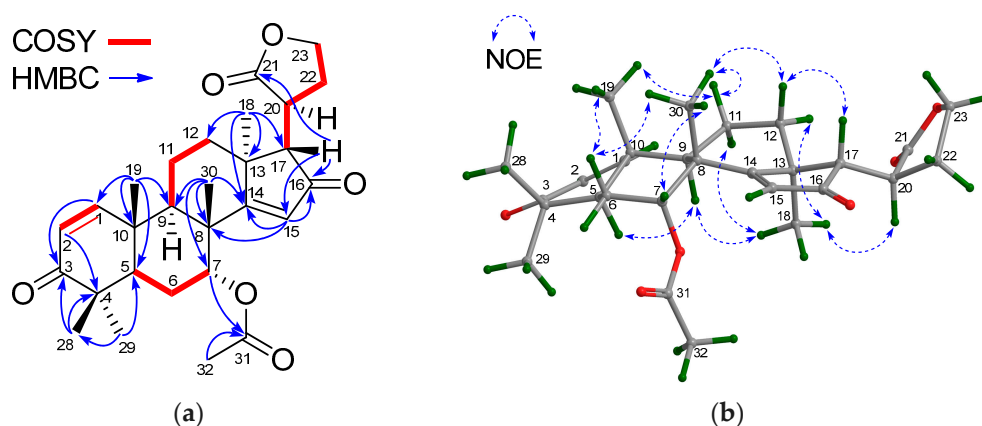


Figure 11. (a) Selected ¹H-¹H COSY and HMBC correlations for compound **28** (measured in CDCl₃); (b) Diagnostic NOE interactions for compound **28** (measured in CDCl₃, MM2-optimized structure).

Compound **29** afforded the molecular formula C₂₇H₃₄O₈ as deduced from the positive HRESIMS ion peak at *m/z* 509.2147 (calcd. for [M + Na]⁺, 509.2146). The NMR spectroscopic data of **29** (Tables 7 and 8) closely resembled those of moluccensin O [25], except for the absence of the 21-OH group, which was corroborated by the upshifted C-21 signal (δ_c 72.4 CH₂ in **29**, δ_c 98.1 CH in moluccensin O) and HMBC correlations from H₂-21 (δ_H 4.85 br d (*J* = 18.3 Hz), 5.03 dd (*J* = 18.3, 2.0 Hz)) to C-20 and C-22. The relative configuration of **29** was assigned as the same as that of moluccensin O based on NOE correlations. Thus, the structure of compound **29**—named xylomolin N—was assigned as 21-dehydroxy-moluccensin O.

The antitumor activities of **1**, **3**, **8**, **10**, **11**, **14**–**16**, **20**, **23**, **25**, and **27** were tested by the MTT cytotoxicity assay against five human tumor cell lines, including human colorectal HCT-8 and HCT-8/T, human ovarian A2780 and A2780/T, and human breast MD-MBA-231 (Table S1) [28]. Cisplatin was used as the positive control. Compounds **11** and **23** showed weak activities against the tested cancer cell lines, whereas the other ten compounds were inactive at 100 μ M. Compound **23** exhibited selective antitumor activity against human breast MD-MBA-231 cancer cells with an IC₅₀ value of 37.7 μ M.

Anti-HIV activities of **1**, **3**, **8**, **10**, **11**, **14**, **20**, **23**–**25**, and **27** were tested *in vitro* with the HIV-1 virus transfected 293 T cells [29]. At the concentration of 20 μ M, **1**, **11**, **23**, and **24** showed inhibitory rates of 17.49 \pm 6.93%, 24.47 \pm 5.04%, 14.77 \pm 5.91%, and 14.34 \pm 3.92%, respectively (Table S2). Efavirenz was used as the positive control with an inhibitory rate of 88.54 \pm 0.45% at the same concentration.

3. Materials and Methods

3.1. General Methods

Optical rotations were recorded on a MCP500 modular circular polarimeter (Anton Paar Opto Tec GmbH, Seelze, Germany). UV spectra were obtained on a GENESYS 10S UV-Vis spectrophotometer (Thermo Fisher Scientific, Shanghai, China). HRESIMS were measured on a Bruker maXis ESI-QTOF mass spectrometer (Bruker Daltonics, Bremen, Germany). NMR spectra were recorded on a Bruker AV-400 spectrometer with TMS as the internal standard. Single-crystal X-ray diffraction analyses were made on an Agilent Xcalibur Atlas Gemini Ultra-diffractometer (Agilent Technologies, Santa Clara, CA, USA) with mirror monochromated CuK α radiation (λ = 1.54178 Å) at 150 K. Semi-preparative HPLC (Waters Corporation, Milford, MA, USA) was performed on a Waters 2535 pump equipped with a waters 2998 photodiode array detector and YMC C18 reverse-phased columns (250 mm \times 10 mm i.d., 5 μ m). For column chromatography, silica gel (100–200 mesh) (Qingdao Mar. Chem. Ind. Co.

Ltd., Qingdao, China) and C₁₈ reverse-phased silica gel (ODS-A-HG 12 nm, 50 µm, YMC Co. Ltd., Kyoto, Japan) were used. ECD spectra were measured on a Jasco J-810 spectropolarimeter (JASCO Corporation, Tokyo, Japan) in MeCN.

3.2. Plant Material

A batch of seeds of *Xylocarpus moluccensis* were collected at the mangrove swamp of Trang Province, Thailand, in June 2013, whereas another batch of seeds of the same mangrove plant were collected in Godavari estuary, Andhra Pradesh, India, in October 2009, respectively. The identification of the plant was performed by one of the authors (J.W.) and Mr. Tirumani Satyanandamurty (Government Degree College at Amadala Valasa, India). Voucher samples (No. ThaiXM-03 and No. IXM200901, respectively) were maintained in the Marine Drugs Research Center, College of Pharmacy, Jinan University.

3.3. Extraction and Isolation

The dried seeds (10.0 kg, ThaiXM-03) of *X. moluccensis* were extracted with 95% (*v/v*) EtOH at room temperature (5 × 20 L) to afford the EtOH extract (680.0 g), which was suspended in water and extracted with EtOAc. The resulting EtOAc extract (296.0 g) was chromatographed on silica gel column and eluted with CHCl₃/MeOH (100:0 to 5:1) to yield 160 fractions.

Fractions 26–28 (31.6 g) were combined and further purified with an RP-18 column (acetone/H₂O, 50:50 to 100:0) to afford 57 subfractions. Subfraction 23 was purified by preparative HPLC (YMC-Pack ODS-5-A, 250 mm × 10 mm i.d., MeOH/H₂O, 50:50) to afford compound **1** (45.0 mg).

Fractions 29–40 (111.0 g) were combined and further purified with an RP-18 column (acetone/H₂O, 50:50 to 100:0) to afford 360 subfractions. The combination of subfractions 90–95 was subjected to preparative HPLC (YMC-Pack ODS-5-A, 250 mm × 10 mm i.d., MeCN/H₂O, 38:62) to give compound **8** (72 mg), along with five other subfractions (SFr.90-95-1 to SFr.90-95-5). Recrystallization of SFr.90-95-1 afforded compound **20** (15.3 mg). Further purification of SFr.90-95-2 with preparative HPLC (YMC-Pack ODS-5-A, 250 mm × 10 mm i.d., MeOH/MeCN/H₂O, 10:40:50) yielded compounds **3** (7.1 mg), **5** (4.3 mg), **12** (37 mg), **13** (2.8 mg), and **21** (1.2 mg), whereas that of SFr.90-95-3 with preparative HPLC (YMC-Pack ODS-5-A, 250 mm × 10 mm i.d., MeOH/H₂O, 60:40 or MeCN/H₂O, 35:65) afforded compounds **6** (4.3 mg) and **9** (3.1 mg). SFr.90-95-4 was further purified with preparative HPLC (YMC-Pack ODS-5-A, 250 mm × 10 mm i.d., MeCN/H₂O, 46:64) to afford compound **14** (57.0 mg). Subfractions 78–83 were combined and further purified by preparative HPLC (YMC-Pack ODS-5-A, 250 × 10 mm i.d., MeOH/H₂O, 50:50) to give compounds **24** (3.5 mg), **26** (2.0 mg), **27** (7.0 mg), and **29** (2.5 mg).

Fractions 157–175 (14.5 g) were combined and further purified with an RP-18 column (acetone/H₂O, 40:60 to 100:0) to afford 45 subfractions. Subfraction 27 was purified by preparative HPLC (YMC-Pack 250 mm × 10 mm i.d., MeCN/MeOH/H₂O, 50:15:35) to afford compound **4** (1.2 mg).

The air-dried seeds (15.0 kg, IXM200901) were powdered and extracted with 95% (*v/v*) EtOH (5 × 20 L) at room temperature to afford the EtOH extract (1.1 kg), which was partitioned between EtOAc and water to afford the EtOAc portion (572.0 g). Then, 252.0 g of the EtOAc extract was further subjected to a silica gel column (105.0 cm × 9.5 cm i.d.) and eluted with a gradient mixture of CHCl₃/MeOH (100:1 to 5:1) to afford 184 fractions.

Fractions 38–43 (26.0 g) were combined and further separated on an RP-18 column (64.0 cm × 6.3 cm i.d.), and eluted with a gradient mixture of acetone/H₂O (40:60 to 100:0) to afford 74 subfractions.

Subfractions 12–16 (1.5 g) were combined and separated by preparative HPLC (YMC-Pack ODS-5-A, 250 mm × 10 mm i.d., MeCN/H₂O, 36:64) to afford seven parts (SFr.12-16-1 to SFr.12-16-7). SFr.12-16-2 was further purified by preparative HPLC (YMC-Pack ODS-5-A, 250 mm × 10 mm i.d., MeOH/H₂O, 49:51) to yield compounds **10** (49.3 mg) and **25** (25.7 mg). SFr.12-16-4 and SFr.12-16-5 were further purified by preparative HPLC (YMC-Pack ODS-5-A, 250 mm × 10 mm i.d., MeOH/H₂O,

52:48) to afford compounds **15** (13 mg) and **22** (3.0 mg), respectively. SFr.12-16-6 was further subjected to preparative HPLC (MeOH/H₂O, 51:49) to yield compound **2** (2.0 mg), whereas SFr.12-16-7 was further purified by preparative HPLC (MeOH/H₂O, 60:40, subsequently with MeCN/H₂O, 60:40, and then MeCN/MeOH/H₂O, 60:20:20) to yield compound **28** (1.5 mg).

Preparative HPLC (YMC-Pack ODS-5-A, 250 mm × 10 mm i.d., MeOH/H₂O, 58:42) was performed on subfraction 27 (2.9 g) to gain compound **16** (4.0 mg). Subfractions 32–35 (1.5 g) were combined and separated by preparative HPLC (YMC-Pack ODS-5-A, 250 mm × 10 mm i.d., MeCN/H₂O, 55:45) to give four parts (SFr.32-35-1 to SFr.32-35-4). SFr.32-35-2 and SFr.32-35-3 were purified by preparative HPLC (MeOH/H₂O, 65:35, MeOH/H₂O, 60:40, respectively) to yield compounds **23** (27.0 mg) and **11** (27.5 mg), respectively, whereas recrystallization (acetone) of SFr.32-35-4 afforded compound **7** (23.8 mg).

Fractions 48–86 (43.9 g) were combined and further performed on an RP-18 column (46.7 cm × 6.4 cm i.d.), and eluted with a gradient mixture of MeCN/H₂O (50:50 to 100:0), to afford 81 subfractions. Subfraction 4 (6.5 g) was purified by preparative HPLC (MeOH/H₂O, 53:47) to yield compound **17** (5.5 mg). Subfractions 8–14 (10.4 g) were combined and further separated on an RP-18 column (62.0 cm × 6.5 cm i.d.) and eluted with a gradient mixture of acetone/H₂O (50:50 to 100:0) to afford 37 subsubfractions, among which subsubfractions 12–15 (2.1 g) were combined and separated on the preparative HPLC (MeOH/MeCN/H₂O, 50:15:35) to give compound **18** (2.1 mg). Subfraction 17 (1.78 g) was subjected to preparative HPLC (MeOH/H₂O, 80:20) to yield compound **19** (1.2 mg).

Xylomolin A₁ (**1**): Colorless crystal; $[\alpha]_D^{25} -62.0$ ($c = 0.06$, acetone); UV (MeCN) λ_{\max} (log ϵ) 199.7 (3.7) nm; ECD (c 0.41 mM, MeCN) λ_{\max} ($\Delta\epsilon$) 190.0 (−12.0), 289.6 (−2.2) nm; ¹H and ¹³C NMR spectroscopic data see Tables 1 and 2; HRESIMS m/z 615.2785 [M + H]⁺ (calcd. for C₃₃H₄₃O₁₁, 615.2800).

Xylomolin A₂ (**2**): White, amorphous powder; $[\alpha]_D^{25} -74.7$ (c 0.04, acetone); UV (MeCN) λ_{\max} (log ϵ) 194.0 (4.5), 279.0 (3.3) nm; ¹H and ¹³C NMR spectroscopic data see Tables 1 and 2; HRESIMS m/z 593.2143 [M + Cl][−] (calcd. for C₃₀H₃₈O₁₀Cl, 593.2159).

Xylomolin A₃ (**3**): White, amorphous solid; $[\alpha]_D^{25} -96.0$ (c 0.05, acetone); UV (MeCN) λ_{\max} (log ϵ) 198.9 (3.9) nm; ECD (c 0.16 mM, MeCN) λ_{\max} ($\Delta\epsilon$) 191.0 (−14.5) nm; ¹H and ¹³C NMR spectroscopic data see Tables 1 and 2; HRESIMS m/z 625.2620 [M + Na]⁺ (calcd. for C₃₂H₄₂NaO₁₁, 625.2619).

Xylomolin A₄ (**4**): White, amorphous powder; $[\alpha]_D^{25} -24.0$ (c 0.08, acetone); UV (MeCN) λ_{\max} (log ϵ) 197.0 (3.9), 201.8 (3.8) nm; ECD (c 0.15 mM, MeCN) λ_{\max} ($\Delta\epsilon$) 190 (−8.1), 200.4 (−5.0), 211.6 (−6.6) nm; ¹H and ¹³C NMR spectroscopic data see Tables 1 and 2; HRESIMS m/z 683.2675 [M + Na]⁺ (calcd. for C₃₄H₄₄NaO₁₃, 683.2674).

Xylomolin A₅ (**5**): White, amorphous powder; $[\alpha]_D^{25} -52.0$ (c 0.04, acetone); UV (MeCN) λ_{\max} (log ϵ) 201.0 (3.8) nm; ECD (c 0.16 mM, MeCN) λ_{\max} ($\Delta\epsilon$) 191.0 (−8.6) nm; ¹H and ¹³C NMR spectroscopic data see Tables 1 and 2; HRESIMS m/z 625.2252 [M + Na]⁺ (calcd. for C₃₁H₃₈NaO₁₂, 625.2255).

Xylomolin A₆ (**6**): White, amorphous powder; $[\alpha]_D^{25} -216.0$ (c 0.10, acetone); UV (MeCN) λ_{\max} (log ϵ) 197.8 (4.0) nm; ECD (c 0.16 mM, MeCN) λ_{\max} ($\Delta\epsilon$) 190.0 (−12.8), 216.4 (+1.5), 294.2 (−2.3) nm; ¹H and ¹³C NMR spectroscopic data see Tables 1 and 2; HRESIMS m/z 609.2311 [M + Na]⁺ (calcd. for C₃₁H₃₈NaO₁₁, 609.2306).

Xylomolin A₇ (**7**): White powder; $[\alpha]_D^{25} -250.7$ (c 0.08, acetone); UV (MeCN) λ_{\max} (log ϵ) 193.0 (4.5) nm; ¹H and ¹³C NMR spectroscopic data see Tables 1 and 2; HRESIMS m/z 593.2358 [M + Na]⁺ (calcd. for C₃₁H₃₈NaO₁₀, 593.2357).

Xylomolin B₁ (**8**): White, amorphous powder; $[\alpha]_D^{25} +212.0$ (c 0.08, acetone); UV (MeCN) λ_{\max} (log ϵ) 204.0 (3.9), 285.4 (4.0) nm; ECD (c 0.10 mM, MeCN) λ_{\max} ($\Delta\epsilon$) 252.1 (−1.6), 278.9 (+8.6) nm; ¹H and ¹³C NMR spectroscopic data see Tables 3 and 4; HRESIMS m/z 607.2151 [M + Na]⁺ (calcd. for C₃₁H₃₆NaO₁₁, 607.2150).

Xylomolin B₂ (9): White, amorphous solid; $[\alpha]_D^{25} +137.0$ (*c* 0.10, acetone); UV (MeCN) λ_{\max} (log ϵ) 207.2 (3.7), 285.2 (4.0) nm; ECD (*c* 0.19 mM, MeCN) λ_{\max} ($\Delta\epsilon$) 190.0 (+3.6), 213.7 (−1.1), 282.2 (+9.5) nm; ¹H and ¹³C NMR spectroscopic data see Tables 3 and 4; HRESIMS *m/z* 527.2273 [M + H]⁺ (calcd. for C₂₉H₃₅O₉, 527.2276).

Xylomolin C₁ (10): White, amorphous powder; $[\alpha]_D^{25} +156.0$ (*c* 0.07, acetone); UV (MeCN) λ_{\max} (log ϵ) 191.0 (4.3), 275 (4.1) nm; ¹H and ¹³C NMR spectroscopic data see Tables 3 and 4; HRESIMS *m/z* 543.2238 [M + H]⁺ (calcd. for C₂₉H₃₅O₁₀, 543.2230).

Xylomolin C₂ (11): White, amorphous powder; $[\alpha]_D^{25} +125.7$ (*c* 0.09, acetone); UV (MeCN) λ_{\max} (log ϵ) 194.0 (4.7), 277 (4.6) nm; ¹H and ¹³C NMR spectroscopic data see Tables 3 and 4; HRESIMS *m/z* 591.2570 [M + Na]⁺ (calcd. for C₃₂H₄₀NaO₉, 591.2565).

Xylomolin D (12): White, amorphous powder; $[\alpha]_D^{25} -34.0$ (*c* 0.05, acetone); UV (MeCN) λ_{\max} (log ϵ) 208.2 (3.8) nm; ECD (*c* 0.16 mM, MeCN) λ_{\max} ($\Delta\epsilon$) 190.0 (−2.6), 217.5 (+13.7), 244.5 (−0.3), 261 (+ 1.5), 291.2 (−3.8) nm; ¹H and ¹³C NMR spectroscopic data see Tables 3 and 4; HRESIMS *m/z* 625.2612 [M + Na]⁺ (calcd. for C₃₂H₄₂NaO₁₁, 625.2619).

Xylomolin E (13): White, amorphous powder; $[\alpha]_D^{25} -68.0$ (*c* 0.04, acetone); UV (MeCN) λ_{\max} (log ϵ) 207.2 (3.9) nm; ECD (*c* 0.15 mM, MeCN) λ_{\max} ($\Delta\epsilon$) 190.0 (−9.5), 213.7 (+2.5) nm; ¹H and ¹³C NMR spectroscopic data see Tables 3 and 4; HRESIMS *m/z* 625.2250 [M + Na]⁺ (calcd. for C₃₁H₃₈NaO₁₂, 625.2255).

Xylomolin F (14): White, amorphous powder; $[\alpha]_D^{25} +4.0$ (*c* 0.03, acetone); UV (MeCN) λ_{\max} (log ϵ) 211.0 (4.1) nm; ECD (*c* 0.21 mM, MeCN) λ_{\max} ($\Delta\epsilon$) 192.0 (−7.1), 219.0 (+4.0), 265.0 (+3.2) nm; ¹H and ¹³C NMR spectroscopic data see Tables 3 and 4; HRESIMS *m/z* 669.2521 [M + Na]⁺ (calcd. for C₃₃H₄₂NaO₁₃, 669.2518).

Xylomolin G₁ (15): White, amorphous solid; $[\alpha]_D^{25} -65.0$ (*c* 0.1, acetone); UV (MeCN) λ_{\max} (log ϵ) 190.2 (4.20) nm; ECD (*c* 0.14 mM, MeCN) λ_{\max} ($\Delta\epsilon$) 207 (+2.3), 238 (−3.8), 290 (+1.4), 321 (−0.32), 344 (+0.32) nm; ¹H and ¹³C NMR spectroscopic data see Tables 5 and 6; HRESIMS *m/z* 587.2494 [M + H]⁺ (calcd. for C₃₁H₃₉O₁₁, 587.2492).

Xylomolin G₂ (16): White, amorphous solid; $[\alpha]_D^{25} -72.0$ (*c* 0.05, acetone); UV (MeCN) λ_{\max} (log ϵ) 190.2 (4.03); ECD (*c* 0.13 mM, MeCN) λ_{\max} ($\Delta\epsilon$) 205.0 (+1.7), 239.0 (−4.3), 302.0 (+0.34), 339.0 (+1.1) nm; ¹H and ¹³C NMR spectroscopic data see Tables 5 and 6; HRESIMS *m/z* 615.2809 [M + H]⁺ (calcd. for C₃₃H₄₃O₁₁, 615.2805).

Xylomolin G₃ (17): White, amorphous solid; $[\alpha]_D^{25} -43.5$ (*c* 0.04, acetone); UV (MeCN) λ_{\max} (log ϵ) 196.6 (4.03), 285.0 (2.93) nm; ECD (*c* 0.15 mM, MeCN) λ_{\max} ($\Delta\epsilon$) 193.0 (−4.5), 197.0 (−3.4), 205.0 (−7.5), 216.0 (−5.0), 233.0 (−7.9), 298 (+4.3) nm; ¹H and ¹³C NMR spectroscopic data see Tables 5 and 6; HRESIMS *m/z* 543.2246 [M + H]⁺ (calcd. for C₂₉H₃₅O₁₀, 543.2230).

Xylomolin G₄ (18): White, amorphous solid; $[\alpha]_D^{25} -44.0$ (*c* 0.01, acetone); UV (MeCN) λ_{\max} (log ϵ) 196.6 (4.08) nm; ECD (*c* 0.18 mM, MeCN) λ_{\max} ($\Delta\epsilon$) 203.0 (−8.7), 215.0 (−6.2), 233.0 (−10.3), 301.0 (+5.0) nm; ¹H and ¹³C NMR spectroscopic data see Tables 5 and 6; HRESIMS *m/z* 555.2593 [M + H]⁺ (calcd. for C₃₁H₃₉O₉, 555.2594).

Xylomolin G₅ (19): White, amorphous solid; $[\alpha]_D^{25} -37.5$ (*c* 0.024, acetone); UV (MeCN) λ_{\max} (log ϵ) 195.0 (4.27), 284.2 (2.86) nm; ECD (*c* 0.11 mM, MeCN) λ_{\max} ($\Delta\epsilon$) 195.0 (+ 0.70), 206.0 (−4.9), 214.0 (−3.5), 231.0 (−6.1), 299.0 (+2.7) nm; ¹H and ¹³C NMR spectroscopic data see Tables 5 and 6; HRESIMS *m/z* 569.2753 [M + H]⁺ (calcd. for C₃₂H₄₁O₉, 569.2751).

Xylomolin H (20): White, amorphous powder; $[\alpha]_D^{25} +65.0$ (*c* 0.06, acetone); UV (MeCN) λ_{\max} (log ϵ) 212.3 (4.0) nm; ECD (*c* 0.16 mM, MeCN) λ_{\max} ($\Delta\epsilon$) 223 (+10.9), 245 (+0.19), 270 (+8.1) nm; ¹H and ¹³C NMR spectroscopic data see Tables 5 and 6; HRESIMS *m/z* 667.2359 [M + Na]⁺ (calcd. for C₃₃H₄₀NaO₁₃, 667.2361).

Xylomolin I (**21**): Light yellow, amorphous gum; $[\alpha]_D^{25} +129.0$ (*c* 0.08, acetone); UV (MeCN) λ_{\max} (log ϵ) 208.4 (3.8), 287.6 (4.1) nm; ECD (*c* 0.17 mM, MeCN) λ_{\max} ($\Delta\epsilon$) 200.0 (+4.6), 213.0 (+2.3), 232.0 (+4.6), 259.0 (−3.9), 291.0 (+10.3) nm; ^1H and ^{13}C NMR spectroscopic data see Tables 5 and 6; HRESIMS m/z 621.2304 $[\text{M} + \text{Na}]^+$ (calcd. for $\text{C}_{32}\text{H}_{38}\text{NaO}_{11}$, 621.2306)

Xylomolin J₁ (**22**): White, amorphous powder; $[\alpha]_D^{25} -135.0$ (*c* 0.11, acetone); UV (MeCN) λ_{\max} (log ϵ) 197.0 (4.9), 213.4 (4.8), 260.8 (4.6) nm; ECD (*c* 0.039 mM, MeCN) λ_{\max} ($\Delta\epsilon$) 204.0 (−3.3), 229.0 (+3.3), 266.0 (+6.3), 310.0 (−0.19), 346.0 (+0.95) nm; ^1H and ^{13}C NMR spectroscopic data see Tables 7 and 8; HRESIMS m/z 541.2077 $[\text{M} + \text{H}]^+$ (calcd. for $\text{C}_{29}\text{H}_{33}\text{O}_{10}$, 541.2074).

Xylomolin J₂ (**23**): White, amorphous powder; $[\alpha]_D^{25} +232.0$ (*c* 0.1, acetone); UV (MeCN) λ_{\max} (log ϵ) 196.8 (5.2), 211.0 (5.1), 260.8 (5.0) nm; ECD (*c* 0.039 mM, MeCN) λ_{\max} ($\Delta\epsilon$) 190.0 (−3.9), 199.0 (−2.0), 206.0 (−2.9), 225.0 (+3.9), 267.0 (+9.1), 310.0 (−0.17), 335.0 (+1.0) nm; ^1H and ^{13}C NMR spectroscopic data see Tables 7 and 8; HRESIMS m/z 583.2548 $[\text{M} + \text{H}]^+$ (calcd. for $\text{C}_{32}\text{H}_{39}\text{O}_{10}$, 583.2543).

Xylomolin K₁ (**24**): White, amorphous powder; $[\alpha]_D^{25} +98.0$ (*c* 0.1, acetone); UV (MeCN) λ_{\max} (log ϵ) 194.0 (4.3), 271.0 (4.3) nm; ECD (*c* 0.33 mM, MeCN) λ_{\max} ($\Delta\epsilon$) 209.0 (+3.0), 211.0 (+2.9), 232.0 (+8.5), 275.0 (−2.8), 300.0 (+6.4) nm; ^1H and ^{13}C NMR spectroscopic data see Tables 7 and 8; HRESIMS m/z 621.2306 $[\text{M} + \text{Na}]^+$ (calcd. for $\text{C}_{32}\text{H}_{38}\text{NaO}_{11}$, 621.2306).

Xylomolin K₂ (**25**): White, amorphous powder; $[\alpha]_D^{25} +120.4$ (*c* 0.07, acetone); UV (MeCN) λ_{\max} (log ϵ) 191.0 (4.3), 272.0 (4.5) nm; ^1H and ^{13}C NMR spectroscopic data see Tables 7 and 8; HRESIMS m/z 607.2164 $[\text{M} + \text{Na}]^+$ (calcd. for $\text{C}_{31}\text{H}_{36}\text{NaO}_{11}$, 607.2150).

Xylomolin L₁ (**26**): White, amorphous powder; $[\alpha]_D^{25} +64.0$ (*c* 0.09, acetone); UV (MeCN) λ_{\max} (log ϵ) 213.0 (4.0) nm; ECD (*c* 0.30 mM, MeCN) λ_{\max} ($\Delta\epsilon$) 220.0 (+12.5), 249.0 (+1.1), 270.0 (+0.8), 236.0 (+1.9) nm; ^1H and ^{13}C NMR spectroscopic data see Tables 7 and 8; HRESIMS m/z 681.2149 $[\text{M} + \text{Na}]^+$ (calcd. for $\text{C}_{33}\text{H}_{38}\text{NaO}_{14}$, 681.2154).

Xylomolin L₂ (**27**): White, amorphous powder; $[\alpha]_D^{25} +42.0$ (*c* 0.06, acetone); UV (MeCN) λ_{\max} (log ϵ) 214 (4.5) nm; ECD (*c* 0.15 mM, MeCN) λ_{\max} ($\Delta\epsilon$) 198.0 (+3.2), 213.0 (−3.6), 234.0 (+11.6) nm; ^1H and ^{13}C NMR spectroscopic data see Tables 7 and 8; HRESIMS m/z 679.2374 $[\text{M} + \text{Na}]^+$ (calcd. for $\text{C}_{34}\text{H}_{40}\text{NaO}_{13}$, 679.2361).

Xylomolin M (**28**): White, amorphous powder; $[\alpha]_D^{25} -252.0$ (*c* 0.03, acetone); UV (MeCN) λ_{\max} 200.0 (4.0), 232 (4.1) nm; ^1H and ^{13}C NMR spectroscopic data see Tables 7 and 8; HRESIMS m/z 469.2603 $[\text{M} + \text{H}]^+$ (calcd. for $\text{C}_{28}\text{H}_{37}\text{O}_6$, 469.2585).

Xylomolin N (**29**): White, amorphous powder; $[\alpha]_D^{25} -17.0$ (*c* 0.05, acetone); UV (MeCN) λ_{\max} (log ϵ) 196 (3.7), 211 (3.7) nm; ECD (*c* 0.21 mM, MeCN) λ_{\max} ($\Delta\epsilon$) 200.0 (−7.0), 224.0 (+2.1), 252.0 (−0.3) nm; ^1H and ^{13}C NMR spectroscopic data see Tables 7 and 8; HRESIMS m/z 509.2147 $[\text{M} + \text{Na}]^+$ (calcd. for $\text{C}_{27}\text{H}_{34}\text{NaO}_8$, 509.2146).

3.4. X-ray Crystal Data for Xylomolin A₁ (**1**)

Orthorhombic, $\text{C}_{34}\text{H}_{46}\text{O}_{12}$ ($\text{C}_{33}\text{H}_{42}\text{O}_{11} \cdot \text{CH}_3\text{OH}$), space group $P2(1)2(1)2(1)$, $a = 8.82730$ (5) Å, $b = 17.93740$ (10) Å, $c = 20.84108$ (13) Å, $\alpha = 90^\circ$, $\beta = 90^\circ$, $\gamma = 90^\circ$, $V = 3299.95$ (3) Å³, $Z = 4$, $D_{\text{calcd.}} = 1.302$ Mg/m³, $\mu = 0.816$ mm^{−1}. Crystal size: $0.40 \times 0.40 \times 0.28$ mm³. 47,329 measured reflections, 5877 [$R_{\text{int}} = 0.0378$] independent reflections, 426 parameters, 0 restraints, $F(000) = 1384.0$, $R_1 = 0.0296$, $wR_2 = 0.0773$ (all data), $R_1 = 0.0286$, $wR_2 = 0.0763$ [$I > 2\sigma(I)$], and goodness-of-fit (F^2) = 1.065. The absolute structural parameter is $-0.06(10)$, Flack x is $-0.14(11)$, and Hooft y is $-0.04(3)$.

CCDC-1590301 (**1**) contains the supplementary crystallographic data for this paper (excluding structure factors). These data are provided free of charge by The Cambridge Crystallographic Data Centre.

3.5. MTT Cytotoxicity Assay

Compounds **1**, **3**, **8**, **10**, **11**, **14–16**, **20**, **23**, **25**, and **27** were evaluated by the MTT method for cytotoxicities against human colorectal HCT-8 and HCT-8/T, ovarian A2780 and A2780/T, and breast MD-MBA-231 cancer cell lines. All cell lines were cultured as adherent monolayers in flasks in DMEM culture medium with 10% fetal bovine serum, benzylpenicillin (50 kU/L), and streptomycin (50 mg/L) at 37 °C in a humidified atmosphere of 5% CO₂. Cells were collected with trypsin and resuspended in a final concentration of 5 × 10⁴/mL. One hundred microliter aliquots for each cell suspension were distributed evenly into 96-well multiplates (number of cells per well is 5 × 10³). Different concentrations of the compounds were added into the designated wells. After 72 h, a 10 µL MTT solution (5 mg/mL) was added to each well, and the plate was further incubated for 4 h, allowing viable cells to reduce the yellow MTT into dark-blue formazan crystals which were dissolved in DMSO 100 µL. The absorbance in individual wells was determined at 490 nm by a microplate reader (Biotek, VT, USA) [28]. The concentrations required to inhibit the growth of cancer cells by 50% (IC₅₀ values) were calculated from cytotoxicity curves by Bliss method. The positive control was cisplatin. The IC₅₀ values of cisplatin in human colorectal HCT-8 and HCT-8/T, ovarian A2780 and A2780/T, and breast MD-MBA-231, were 15.43, 21.98, 8.54, 9.26, and 6.25 µM, respectively.

3.6. HIV-Inhibitory Bioassay

For the assay, 293 T cells (2 × 10⁵) were co-transfected with 0.6 µg of pNL-Luc-E⁻-Vpu⁻ and 0.4 µg of vesicular stomatitis virus glycoprotein (VSV-G) expression vector pHIT/G. After 48 h, the VSV-G pseudotyped viral supernatant (HIV-1) was harvested by filtration through a 0.45-µm filter and the concentration of viral capsid protein was determined by p24 antigen capture ELISA (Biomerieux, Shanghai, China). SupT1 cells were exposed to VSV-G pseudotyped HIV-1 (multiplicity of infection (MOI) = 1) at 37 °C for 48 h in the absence or presence of the test compounds (**1**, **3**, **8**, **10**, **11**, **14**, **20**, **23–25**, and **27**). Efavirenz was used as the positive control. The inhibition rates were determined by using a firefly Luciferase Assay System (Promega, Madison, WI, USA) [29].

4. Conclusions

Twenty-nine new limonoids were isolated from the seeds of the mangrove plant, *Xylocarpus moluccensis*, collected in Thailand and India. The structures of these limonoids, including absolute configurations of ten compounds, *viz.* **1**, **15–19**, **21–23**, and **26**, were established by HRESIMS, extensive NMR investigations, single-crystal X-ray diffraction analysis conducted with Cu K α radiation, and the comparison of experimental ECD spectra. Compounds **1–14** are mexicanolides, whereas **15–21** are khayanolides. Compounds **22** and **23** are unusual limonoids possessing a (*Z*)-bicyclo[5.2.1]dec-3-en-8-one motif, while **24** and **25** are 30-ketophragmalins. Compounds **26** and **27** are phragmalin 8,9,30-*ortho* esters, whereas **28** and **29** are azadirone and andirobin derivatives. These results demonstrate that *X. moluccensis* continues to be an abundant resource for the production of novel limonoids with structural diversity. Compound **23** exhibited selective antitumor activity against human triple-negative breast MD-MBA-231 cancer cells with an IC₅₀ value of 37.7 µM, whereas compounds **1**, **11**, **23**, and **24** showed inhibitory rates of 17.49 ± 6.93%, 24.47 ± 5.04%, 14.77 ± 5.91%, and 14.34 ± 3.92% against HIV-I virus, respectively, at the concentration of 20 µM.

Supplementary Materials: The following are available online at www.mdpi.com/1660-3397/16/1/38/s1. Table S1: Cytotoxic assay results for compounds against human cancer cells; Table S2: HIV-inhibitory bioassay results for tested compounds; Copies of HRESIMS of compounds **1–29**, and 1D and 2D NMR spectra of compounds **1–29**.

Acknowledgments: This work was financially supported by NSFC (U1501221, 31770377, 81661148049, and 81125022), the Pearl River S&T Nova Program of Guangzhou, China (201506010023), the Science and Technology Planning Project of Guangdong Province, China (2013B051000057), and the Fundamental Research Funds for the Central Universities, China (21617474). We thank Tirumani Satyanandamurty (Government Degree College at Amadala Valasa, India) and Patchara Pedpradab (Rajamangala University of Technology Srivijaya, Trang Province, Thailand) for providing the plant materials in this work.

Author Contributions: Li Shen and Jun Wu conceived and designed the experiments; Jianzhi Zhang, Wanshan Li, and Yiguo Dai performed the experiments and analyzed the data; Jianzhi Zhang and Wanshan Li wrote the draft; Li Shen and Jun Wu revised the paper. All authors have read and approved the manuscript.

Conflicts of Interest: The authors declare no conflict of interest.

References

1. Tan, Q.G.; Luo, X.D. Meliaceous limonoids: Chemistry and biological activities. *Chem. Rev.* **2011**, *111*, 7437–7522. [[CrossRef](#)] [[PubMed](#)]
2. Fang, X.; Di, Y.T.; Hao, X.J. The advances in the limonoid chemistry of the *Meliaceae* family. *Curr. Org. Chem.* **2011**, *15*, 1363–1391.
3. Gualdani, R.; Cavalluzzi, M.M.; Lentini, G.; Habtemariam, S. The chemistry and pharmacology of citrus limonoids. *Molecules* **2016**, *21*, 1530. [[CrossRef](#)] [[PubMed](#)]
4. Jolanta, P.; Jan, S.D.; Agata, K.; Stanislaw, L. Variability of biological activities of limonoids derived from plant sources. *Mini-Rev. Org. Chem.* **2014**, *11*, 269–279. [[CrossRef](#)]
5. Ye, F.; Li, X.W.; Guo, Y.W. Recent progress on the mangrove plants: Chemistry and bioactivity. *Curr. Org. Chem.* **2016**, *20*, 1923–1942. [[CrossRef](#)]
6. Wu, J.; Xiao, Q.; Xu, J.; Li, M.Y.; Pan, J.Y.; Yang, M.H. Natural Products from True Mangrove Flora: Source, Chemistry and Bioactivities. *Nat. Prod. Rep.* **2008**, *25*, 955–981. [[CrossRef](#)] [[PubMed](#)]
7. Rajab, M.S.; Rugutt, J.K.; Fronczek, F.R.; Fischer, N.H. Structural Revision of Harrisonin and 12 β -Acetoxylharrisonin, Two Limonoids from *Harrisonia abyssinica*. *J. Nat. Prod.* **1997**, *60*, 822–825. [[CrossRef](#)]
8. Shen, L.R.; Dong, M.; Yin, B.W.; Guo, D.; Zhang, M.L.; Shi, Q.W.; Huo, C.H.; Kiyota, H.; Suzuki, N.; Cong, B. Xylomexicanins A and B, New $\Delta^{14,15}$ -Mexicanolides from Seeds of the Chinese Mangrove *Xylocarpus granatum*. *Z. Naturforschung C* **2009**, *64*, 37–42. [[CrossRef](#)]
9. Zhou, Z.F.; Kurtán, T.; Mándi, A.; Gu, Y.C.; Yao, L.G.; Xin, G.R.; Li, X.W. Novel and neuroprotective tetranortriterpenoids from Chinese mangrove *Xylocarpus granatum* Koenig. *Sci. Rep.* **2016**, *6*, 33908–33918. [[CrossRef](#)] [[PubMed](#)]
10. Lakshmi, V.; Mishra, V.; Palit, G. A new gastroprotective effect of limonoid compounds xylocensins X and Y from *Xylocarpus moluccensis* in rats. *Nat. Prod. Bioprospect.* **2014**, *4*, 277–283. [[CrossRef](#)] [[PubMed](#)]
11. Yin, X.; Li, X.; Hao, Y.G.; Zhao, Y.W.; Zhou, J.H.; Shi, H.S. Xylocarpin H, a Limonoid of *Xylocarpus granatum*, Produces Antidepressant-Like Activities in Mice. *J. Behav. Brain Sci.* **2015**, *5*, 524–532. [[CrossRef](#)]
12. Connolly, J.D.; Maclellan, M.; Okorie, D.A.; Taylor, D.A.H. Limonoids from *Xylocarpus moluccensis* (Lam.) M. Roem. *J. Chem. Soc. Perkin Trans. 1* **1976**, 1993–1996. [[CrossRef](#)]
13. Taylor, D.A.H. Limonoid extractives from *Xylocarpus moluccensis*. *Phytochemistry* **1983**, *22*, 1297–1299. [[CrossRef](#)]
14. Mulholland, D.A.; Taylor, D.A.H. Limonoids from Australian members of the meliaceae. *Phytochemistry* **1992**, *31*, 4163–4166. [[CrossRef](#)]
15. Li, W.S.; Wu, J.; Li, J.; Satyanandamurty, T.; Shen, L.; Bringmann, G. Krishnadimer A, an axially chiral non-biaryl natural product: Discovery and biomimetic synthesis. *Org. Lett.* **2017**, *19*, 182–185. [[CrossRef](#)] [[PubMed](#)]
16. Li, W.S.; Shen, L.; Bruhn, T.; Pedpradab, P.; Wu, J.; Bringmann, G. Trangmolins A–F with an unprecedented structural plasticity of the rings A and B: New insight into limonoid biosynthesis. *Chem. Eur. J.* **2016**, *22*, 11719–11727. [[CrossRef](#)] [[PubMed](#)]
17. Dai, Y.G.; Li, W.S.; Pedpradab, P.; Liu, J.J.; Wu, J.; Shen, L. Thaxylomolins O–R: Four new limonoids from the Trang mangrove, *Xylocarpus moluccensis*. *RSC Adv.* **2016**, *6*, 85978–85984. [[CrossRef](#)]
18. Li, W.S.; Jiang, Z.P.; Shen, L.; Pedpradab, P.; Bruhn, T.; Wu, J.; Bringmann, G. Antiviral limonoids including khayanolides from the Trang mangrove plant *Xylocarpus moluccensis*. *J. Nat. Prod.* **2015**, *78*, 1570–1578. [[CrossRef](#)] [[PubMed](#)]
19. Yuan, T.; Zhang, C.R.; Yang, S.P.; Yue, J.M. Limonoids and Triterpenoids from *Khaya senegalensis*. *J. Nat. Prod.* **2010**, *73*, 669–674. [[CrossRef](#)] [[PubMed](#)]
20. Li, J.; Li, M.Y.; Feng, G.; Zhang, J.; Karonen, M.; Sinkkonen, J.; Satyanandamurty, T.; Wu, J. Moluccensins R–Y, Limonoids from the Seeds of a Mangrove, *Xylocarpus moluccensis*. *J. Nat. Prod.* **2012**, *75*, 1277–1283. [[CrossRef](#)] [[PubMed](#)]

21. Yang, W.; Kong, L.M.; Li, S.F.; Li, Y.; Zhang, Y.; He, H.P.; Hao, X.J. Five new mexicanolide type limonoids from *Heynea trijuga*. *Nat. Prod. Bioprospect.* **2012**, *2*, 145–149. [[CrossRef](#)]
22. Lin, B.D.; Yuan, T.; Zhang, C.R.; Dong, L.; Zhang, B.; Wu, Y.; Yue, J.M. Structurally Diverse Limonoids from the Fruits of *Swietenia mahagoni*. *J. Nat. Prod.* **2009**, *72*, 2084–2090. [[CrossRef](#)] [[PubMed](#)]
23. Sarigaputi, C.; Sommit, D.; Teerawatananond, T.; Pudhom, K. Weakly anti-inflammatory limonoids from the seeds of *Xylocarpus rumphii*. *J. Nat. Prod.* **2014**, *77*, 2037–2043. [[CrossRef](#)] [[PubMed](#)]
24. Ohtani, I.; Kusumi, T.; Kashman, Y.; Kakisawa, H. High-field FT NMR application of Mosher's method. The absolute configurations of marine terpenoids. *J. Am. Chem. Soc.* **1991**, *113*, 4092–4096. [[CrossRef](#)]
25. Wu, J.; Yang, S.X.; Li, M.Y.; Feng, G.; Pan, J.Y.; Xiao, Q.; Sinkkonen, J.; Satyanandamurty, T. Limonoids and Tirucallane Derivatives from the Seeds of a Krishna Mangrove, *Xylocarpus moluccensis*. *J. Nat. Prod.* **2010**, *73*, 644–649. [[CrossRef](#)] [[PubMed](#)]
26. Abdelgaleil, S.A.; Doe, M.; Morimoto, Y.; Nakatani, M. Rings B,D-*seco* limonoids from the leaves of *Swietenia mahogani*. *Phytochemistry* **2006**, *67*, 452–458. [[CrossRef](#)] [[PubMed](#)]
27. Sakamoto, A.; Tanaka, Y.; Tanaka, R. Andirolides Q-V from the flower of andiroba (*Carapa guianensis*, Meliaceae). *Fitoterapia* **2013**, *90*, 20–29. [[CrossRef](#)] [[PubMed](#)]
28. Jiang, Q.W.; Cheng, K.J.; Mei, X.L.; Qiu, J.G.; Zhang, W.J.; Xue, Y.Q.; Qin, W.M.; Yang, Y.; Zheng, D.W.; Chen, Y.; et al. Synergistic anticancer effects of triptolide and celastrol, two main compounds from thunder god vine. *Oncotarget* **2015**, *6*, 32790–32804. [[CrossRef](#)] [[PubMed](#)]
29. Zhang, Q.; Liu, Z.L.; Mi, Z.Y.; Li, X.Y.; Jia, P.P.; Zhou, J.M.; Yin, X.; You, X.F.; Yu, L.Y.; Guo, F.; et al. High-throughput assay to identify inhibitors of Vpu-mediated down-regulation of cell surface BST-2. *Antivir. Res.* **2011**, *91*, 321–329. [[CrossRef](#)] [[PubMed](#)]



© 2018 by the authors. Licensee MDPI, Basel, Switzerland. This article is an open access article distributed under the terms and conditions of the Creative Commons Attribution (CC BY) license (<http://creativecommons.org/licenses/by/4.0/>).